Comparative study between ZN PID, GA based PID and ANFIS PD controller to a shell and tube heat exchanger temperature control system

Melat Getachew Kebede

A Thesis Submitted to

The Department of Electrical Power and Control Engineering

School of Electrical Engineering and Computing

Presented in Partial Fulfillment of the Requirement for the Degree of Master's in Electrical Power and Control Engineering (Control Engineering)

Office of Graduate Studies

Adama Science and Technology University

June 2022

Adama, Ethiopia

Comparative study between PID, GA based PID and ANFIS PD controller to a shell and tube heat exchanger temperature control system

Melat Getachew Kebede

Advisor: Dr. Tafese Asrat

A Thesis Submitted to

The Department of Electrical Power and Control Engineering

School of Electrical Engineering and Computing

Presented in Partial Fulfillments of the Requirement for the Degree of Master's in Electrical Power and Control Engineering (Control Engineering)

Office of Graduate Studies

Adama Science and Technology University

June 2022

Adama, Ethiopia

DECLARATION

I hereby declare that this Master Thesis entitled “Comparative study between ZN PID, GA based PID and ANFIS PD controller to a shell and tube heat exchanger temperature control system" is my original work. That is, it has not been submitted for the award of any academic degree, diploma, or certificate in any other university. All sources of materials that are used for this thesis have been duly acknowledged through citation.

Melat Getachew Kebede _____ _____

Name of student Signature Date

RECOMMENDATION

I, the advisor of this thesis, hereby certify that I have read the revised version of the thesis entitled " Comparative study between ZN PID, GA based PID and ANFIS PD controller to a shell and tube heat exchanger temperature control system," prepared under my guidance by Melat Getachew Kebede, submitted in partial fulfillment of the requirements for the degree of Masters of Science in Control Engineering. Therefore, I recommend the submission of a revised version of the thesis to the department following the applicable procedures.

Dr. Tafesse Asrat _____ _____

Major Advisor Signature Date

APPROVAL SHEET

I, the advisors of the thesis entitled “Comparative study between ZN PID, GA based PID and ANFIS PD controller to a shell and tube heat exchanger temperature control system “developed by Melat Getachew Kebede, hereby certify that the recommendation and suggestions made by the board of examiners are appropriately incorporated into the final version of the thesis.

Dr. Tafesse Asrat _____ _____ _____

Major Advisor/supervisor Signature Date

We, the undersigned, members of the Board of Examiners of the thesis by Melat Getachew, have read and evaluated the thesis entitled " Comparative study between ZN PID, GA based PID and ANFIS PD controller to a shell and tube heat exchanger temperature control system " and examined the candidate during the open defense. This is, therefore, to certify that the thesis is accepted for partial fulfillment of the requirement of the degree of Master of Science in Control Engineering.

_____ _____ _____

Chairperson Signature Date

_____ _____ _____

Internal Examiner Signature Date

_____ _____ _____

External Examiner Signature Date

Finally, approval and acceptance of the thesis is contingent upon submission of its final copy to the Office of Postgraduate Studies (OPGS) through the Department of Graduate Council (DGC) and School Graduate Committee (SGC).

_____ _____ _____

Department Head Signature Date

_____ _____ _____

School Dean Signature Date

_____ _____ _____

Office of Postgraduate Studies, Dean Signature Date

ACKNOWLEDGEMENT

Words cannot express my gratitude to the almighty God who gave me patience, strength, and courage from the beginning to the completion of the thesis.

I am extremely grateful to my advisor, **Dr. Tafesse Asrat**. For his invaluable advice, inspiration, support, and continued encouragement during the journey of this thesis. His advice and guidance carried me through all the stages of writing my thesis.

I would also like to express my deepest gratitude to **Dr. Tefera Yetayew** for sharing his immense knowledge with me during my successive progress reports. His generous advice, feedback, and support have helped me a lot.

Moreover, I am deeply indebted to the EPCE department head, **Mr. Mesfin Megra (MSc.),** for his humble cooperation at the time I needed support from the department.

Lastly, I would be remiss in not mentioning my father. The belief he has in me motivated me and improved my confidence during the journey of the thesis.

ABSTRACT

A heat exchanger device is widely used in process industries because it is capable of sustaining a wide range of temperatures. The main purpose of a heat exchanger is to transfer heat from a hot fluid to a cooler fluid so that the temperature of the process fluid is controlled. Among the different heat exchanger types, shell and tube heat exchanger is the most commonly used type in the process industry. The heat exchanger temperature control system is a highly nonlinear, uncertain, time-delayed, and complex system. In addition to that, it is accompanied by the presence of two predominant disturbances, namely flow variation and temperature variation of input fluid. In this thesis, the performance of Ziegler–Nichols based proportional integral and derivative controller, genetic algorithm based proportional integral and derivative controller, and adaptive neuro fuzzy inference system has been analyzed and compared under four scenarios, namely no disturbance, flow variation disturbance, temperature variation disturbance, and both disturbance conditions. Among the proposed controllers adaptive neuro fuzzy inference system has provided the best transient response performance with and without the presence of disturbance effects. The settling time of the adaptive neuro fuzzy inference system for the proposed system under no disturbance, flow disturbance, temperature disturbance, and both disturbance conditions is 25.045sec, 25.439sec, 26.948sec, and 27.932sec. It has been improved by 54.9%, 55.2%, 52.8%, and 52.1% when compared to the Ziegler–Nichols tuned proportional integral and derivative controller. And the percentage overshoot of the adaptive neuro fuzzy inference system for the proposed system under no disturbance, flow disturbance, temperature disturbance, and both disturbance conditions is 0.901%, 0.462%, 0.1226%, and 0.00012% %. On the other hand, among the three objective functions used the overall performance of genetic algorithm based proportional integral and derivative controller tuned based on minimizing time integral of absolute error objective function is better than the one tuned based on minimizing integral of absolute error and integral of squared error objective functions.

***Key words**: ZN tuned PID controller, GA tuned PID controller, ANFIS PD controller, and shell and tube heat exchanger*

TABLE OF CONTENTS

LIST OF TABLES

LIST OF FIGURES

LIST OF ACRONYMS

ANFIS	Adaptive Neuro Fuzzy Inference System
ANN	Artificial Neural Network
CV	Controlled Variable
DV	Disturbance Variable
FIS	Fuzzy Inference System
FLC	Fuzzy Logic Controller
FOPID	First Order Pulse Dead Time
GA	Genetic Algorithm
HE	Heat Exchanger
IAE	Integral Absolute Error
ISE	Integral Square Error
ITAE	Integral of Time Absolute Error
LMTD	Log Mean Temperature Difference
MF	Membership function
MV	Manipulated Variable
NN	Neural Network
RTD	Resistive Temperature Detectors
STHE	Shell and Tube Heat Exchanger
TF	transfer function
T-S	Takagi Sugeno
ZN	Ziegler–Nichols

CHAPTER ONE

1. INTRODUCTION

1.1. Background of the Thesis

A heat exchanger (HE) is a thermal device used in process industries as a medium to transfer heat energy (enthalpy) from hot fluid to cooler fluid so that the targeted temperature of the process fluid is attained (Vasičkaninová et al., 2020). The mechanism through which the transfer of energy takes place is indirect; there is no direct physical contact between the two fluids (ThayaaSree et al., 2021). The HE device plays an important role in many industries, such as nuclear power plants, petrochemicals, sewage treatment, food processing, beverage, chemical, petroleum refineries, pharmaceutical sectors, natural gas processing, etc. These devices are crucial in the process industry, which has attracted the attention of many researchers in studying HE system control (Tridianto et al., 2017).

Despite the availability of different heat exchangers, shell and tube heat exchangers are the most commonly used in most industries (ThayaaSree et al., 2021). This is due to their availability, mechanical robustness, flexibility, compact structure, and ability to provide various ranges of temperature and pressure (Valarmathi, 2018) (Somasundar Reddy & Balaji, 2020). In the STHE system, the manipulated (controlling) fluid flows through the tube side and the controlled fluid flows through the shell side of the STHE (Dodd, 1983). A typical picture of industrial STHE is represented in figure 1.1.

Figure 1. 1 Physical appearance of industrial shell and tube heat exchanger plant

Regulatory issues are very common in the chemical industry (Seborg, 2017). The regulatory issue concerned with disturbance rejection. That means, in regulatory issues, the

control objective is to maintain the controlled variable at a fixed desired value despite the presence of disturbance. The STHE temperature control system is expected to address the regulatory issue by maintaining the temperature of the process fluid at the desired set point despite the change in temperature variation and flow variation of the input fluid.

The heat exchanger system is a highly nonlinear, uncertain, time-delayed, and complex system. In addition to that, it is accompanied by the presence of two predominant disturbances, namely: flow variation of the input fluid and temperature variation of the input fluid (Abdullah, 2019). Achieving desired system performance despite these challenges, forced control engineers to design an advanced control strategy (Khames et al., 2020).

Numerous control strategies were proposed to solve the difficulties in the STHE control system. Some of them include internal model controllers, sliding mode controllers (SMC), feed-forward plus feedback controllers, intelligent controllers, and other controllers. The contributions that have been made by other researchers will be discussed in the literature review section of this thesis. Among the proposed controllers, the intelligent controller provides better performance. And many researchers have shown the effectiveness of an intelligent controller in the chemical and production industries (Dutta & Upreti, 2021).

For the last two decades, the intelligence-based approach has been acting as an effective solution for a variety of applications. One of the best characteristics of an intelligent controller is its capability to achieve controllability and robustness by dealing with non-linearity and uncertainty, which is very common in the process industry (Jamal & Syahputra, 2016) (Dutta & Upreti, 2021). The idea of an intelligent controller is based on the fact that assimilating the three intelligent features of human beings, namely learning, adaptation, and reasoning, into a control structure so that the intelligent behavior of a human being is emulated by the control decision mechanism.

In this thesis, comparative studies of classical PID, GA based PID and ANFIS PD have been conducted for a STHE temperature control system. In GA-based PID, the parameters of proportional, integral, and derivative gains are tuned using three different objective functions so that industries can choose based on the performance they need to achieve. An ANFIS PD controller is designed in such a way that first the GA tuned PID controller is used so that training data sets are obtained. The data sets that are taken for ANFIS training

are error, rate of change of error, and control signal. Once the training has been completed, the obtained FIS file from the ANFIS structure is implemented to control the proposed system. The complete simulation of the system and controller was developed using MATLAB/2019a.

1.2. Statement of the problem

HE is a critical device in the process industry; it is used to preheat and pasteurize the process variable. Such activities are achieved within certain ranges of temperature and affect the flavor, shelf life, nutritional content, and quality of the product. Even though the device is related to safety, industries are still using a classical PID controller to control the temperature of the exchanger device. Since the PID controller is a linear system control method, it may not achieve good performance for highly nonlinear systems like the HE temperature control system. The demerits of the traditional PID controller to the proposed system are discussed in the following paragraph.

A heat exchanger temperature control system is a highly nonlinear and uncertain system; it is difficult to achieve the desired performance using a classical PID controller. In addition to nonlinearity problems, the system also exhibits significant time-delayed behavior. The time delays make the temperature loop hard to tune using a classical PID controller, and therefore the system needs an advanced control strategy. While PID control is a crisp control, tuning of the P, I, and D parameters is quite difficult, and the resultant response has a high percentage of overshoot, oscillation, and longer settling time, which is undesirable.

1.3. The objective of the study

1.3.1. General objective

The general objective of this thesis is to perform a comparative study between ZN PID, GA-based PID, and the ANFIS PD controller for a STHE temperature control system.

1.3.2. Specific objective

- ✓ Studding the dynamic model of the exchanger plant, sensor and the control valve
- ✓ To design ZN-tuned PID, GA-tuned PID, and ANFIS PD controllers for a STHE temperature control system.

- ✓ To simulate the response of the system with the proposed controllers in MATLAB/Simulink.
- ✓ To evaluate the performance of the ZN-tuned PID, GA-tuned PID, and ANFIS PD controllers with and without disturbance.
- ✓ To compare the performance of the proposed controllers in terms of transient and error based criteria.
- ✓ To recommend the best controller among the proposed controllers.

1.4. Scope of the study

This thesis focuses on studying modeling and simulation design of the STHE temperature control system. The modeled system is then controlled by three different controllers: ZN tuned PID, GA tuned PID, and ANFIS PD. Finally, the performance of the proposed controllers is evaluated and compared in terms of error-based and transient response criteria.

1.5. Limitation of the study

The parameters for the proposed system are not directly taken from the industries. Instead, they are taken from the literature survey conducted on the related work. This is due to the fact that all the demanded data are not obtained from the industry.

1.6. Motivation of the study

Process control is one of the most active research areas in the field of control engineering. Among the variables that are controlled in the process industry, temperature control is the most crucial because it is related to human health, nutritional content, and the quality of the product. Moreover, most activities in the process industry are performed within a certain range of temperature. HE temperature control is an example of process control in which different control methods can be implemented. Practically, the HE device is indispensable in the food processing industry, sewage treatment, natural gas processing, petrochemical, sewage treatment, beverage, chemical, and pharmaceutical sectors. An appropriate controller has to be designed for optimal operation of the system in the mentioned sector. Different controllers can be implemented based on the needs of the industry.

1.7. Significance of the study

The HE device is indispensable in the food processing industry, petrochemical, beverage, chemical, and pharmaceutical sectors. All the mentioned sectors demand better quality of their products. In order to get such advantages, they need a better control strategy. This thesis is significant in dealing with the difficulties of temperature control in the STHE temperature control system. Moreover, this thesis is significant in helping industries choose the best controller based on the performance they need to achieve.

1.8. Thesis organization

This thesis work has been structured into five chapters. The backgrounds of the study, the statement of the problem, the objective, scope, significance, motivation, and limitations of the study have been presented in the first chapter. Literature surveys in terms of understanding the basic theory and working principles as well as gap findings have been conducted in the second chapter. The methodologies that have been followed are presented in the third chapter. In the fourth chapter, the designed controllers and tuning algorithms are presented. In the fifth chapter, the simulation results and performance comparisons among the proposed controllers have been presented. Finally, the conclusion that has been drawn and a possible recommendation for future work have been presented.

CHAPTER TWO

2. LITERATURE REVIEW

In this chapter, the background study in terms of understanding the basic concept and gap findings has been completed so that the thesis work is accomplished. The heat transfer mechanism utilized by the heat exchanger device is reviewed. The classification of HE devices and the advantages of STHE over the other types are discussed. The working principles of the temperature sensor, control valve, heat exchanger devices, and other components of HE temperature control are also discussed. Finally, related journals and articles have been reviewed with respect to their strong and weak sides. And the contribution made by this thesis is also discussed.

2.1. Heat transfer mechanisms

The heat transfer mechanisms are categorized as conduction, convection, and radiation. In conduction, heat energy is transferred due to molecular contact. In convection, heat energy is transferred as a result of density differences. In radiation, heat energy is transferred by electromagnetic waves (Lavine, 2017).

2.1.1. Conduction

Conduction is one of the heat transfer mechanisms that transfers thermal energy as a result of molecular contact between adjacent molecules. In the conduction mechanism, a molecule that has higher molecular (thermal) energy transfers thermal energy to an adjacent molecule that has lower thermal energy (Lavine, 2017).

2.1.2. Convection

Convection is a heat-transferring mechanism that transfers heat energy as a result of fluid movement. The fluid can be either liquid or gas. The faster the fluid moves, the greater the heat transfer rate by convection. This mechanism of heat transfer occurs due to a density difference, which results from a temperature difference. In such a heat transfer mechanism, the hotter fluid near the heater rises, whereas the cold fluid sinks (Lavine, 2017).

2.1.3. Radiation

Radiation transmits heat energy in the form of electromagnetic waves through empty space. This mechanism of heat transfer occurs as a result of wave motion, doesn't require any material for heat to travel, and can occur in an open and empty space. An example of such a transfer mechanism is the heat energy transferred from sun to the earth (Lavine, 2017).

2.1.4. Heat transfer mechanism of heat exchanger system

The heat exchanger uses conduction and convection so that heat energy is transferred between two fluids. This is achieved based on the principle that heat energy is transferred by convection from the hotter fluid to the separating medium, which separates the two fluids. Then the separating medium conducts energy to the other side of it by conduction. Finally, the cooler fluid takes away heat energy from the separating wall by convection (Lavine, 2017)**.** The driving force for heat energy transfer in an HE device is temperature deviation. This temperature deviation is expressed in terms of a log mean temperature difference (LMTD). The greater the LMTD, the more heat will be transferred. For a better understanding of LMTD, let us take a look at figure 2.1(Khan, 2017).

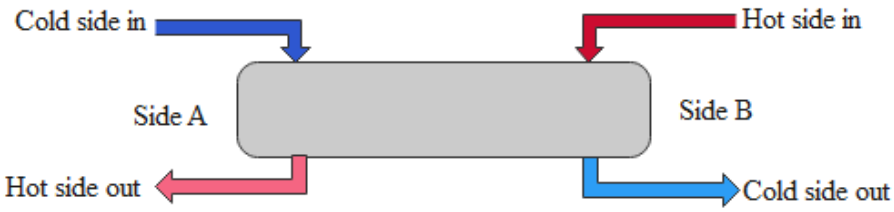

Figure 2. 1 Log mean temperature difference

The LMTD is represented by the equation below.

$$LMTD = \frac{\Delta T_A - \Delta T_B}{\log\left(\frac{\Delta T_A}{\Delta T_B}\right)} \tag{2.1}$$

Where $, \Delta T_A$ is a difference in temperature for side A, and ΔT_B is a difference in temperature for side B.

2.2 Heat exchanger classification

Heat exchangers are classified according to construction, flow arrangement, transfer process, phase of the fluid, etc. The basic heat exchanger classifications are shown in figure 2.2 (Padhee, 2014).

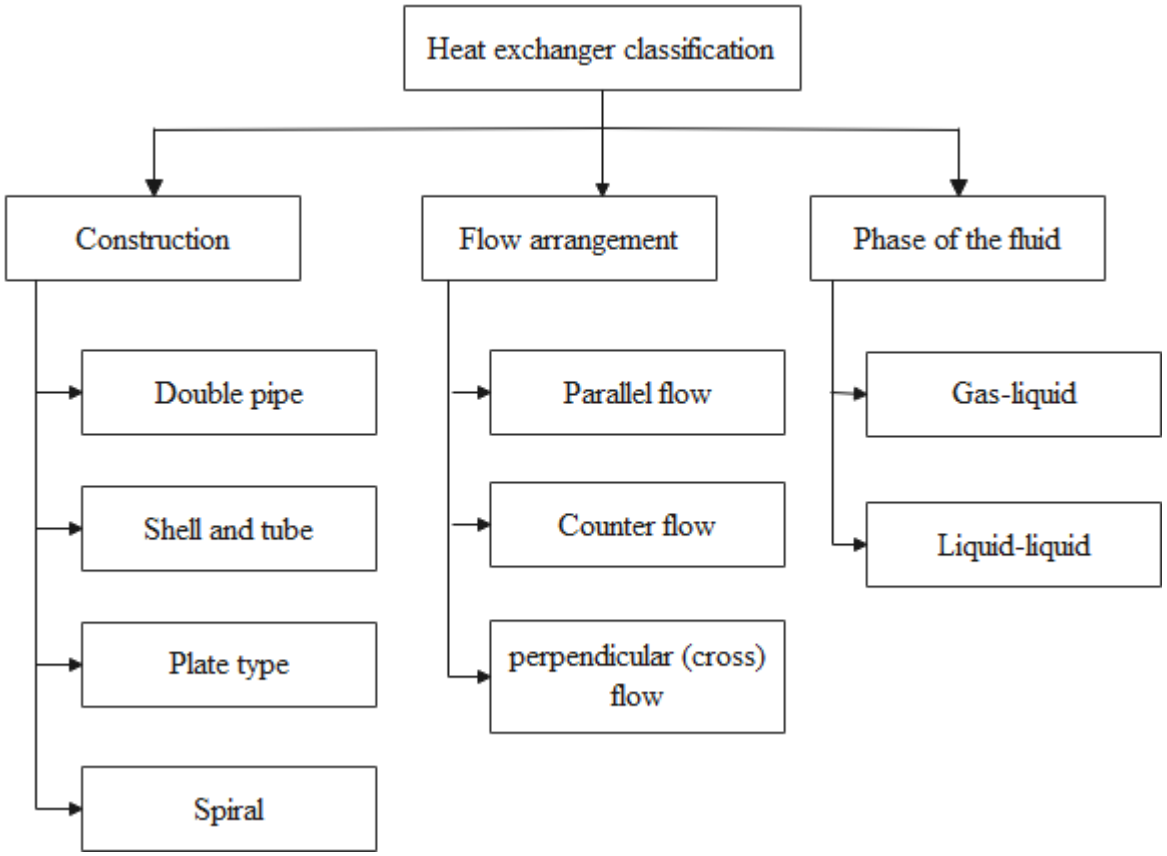

Figure 2. 2 Heat exchanger classifications

The temperature range, pressure range, thermal performance, safety issues, pressure drop, corrosion tendency, inspection possibility, operating cost and capital, cleanability, cross-sectional area they provide for heat transfer, mechanical robustness, availability, exposure to failure, and fouling issues all play a role in HE device selection .

2.2.1. Classification according to flow arrangement

Classification is based on the direction in which the fluids flow. In this aspect, the heat exchanger device is classified as a parallel flow, counter flow, and perpendicular (cross) flow (Bastida et al., 2019) (Khames et al., 2020).

- Parallel flow: In such a flow arrangement of the heat exchanger, the two fluids (hot and cold) have the same direction of flow, enter at the same end, and leave at the same end.
- Counter flow: In such a flow arrangement of the HE devices, the two fluids flow in the opposite direction, enter at different ends, and leave at different ends. Such a flow arrangement minimizes thermal stress and provides a uniformly distributed heat transfer rate.
- Perpendicular flow: In such a flow arrangement of the HE device, the two fluids flow perpendicularly to each other.

Among the three flow arrangements, the counter flow arrangement is the best for heat transfer applications. This is due to the fact that in this flow arrangement, the created temperature difference is large along any unit length and the impact of the thermal stress is minimized (Vasickaninová & Bakošová, 2015).

2.2.2. Classification according to construction

Double pipe heat exchanger: Double pipe HE is a device that exchanges heat through a concentric wall. Such HEs are simple and require less maintenance and design costs. However, they have less efficiency and a smaller diameter. Additionally, the amount of space they occupy is large when compared to the other types of HE devices. This adverse effect has made them unusable in modern industries. Such devices are mostly used in cases where the required heat transfer surface area is small (Lavine, 2017)(Khan, 2017).

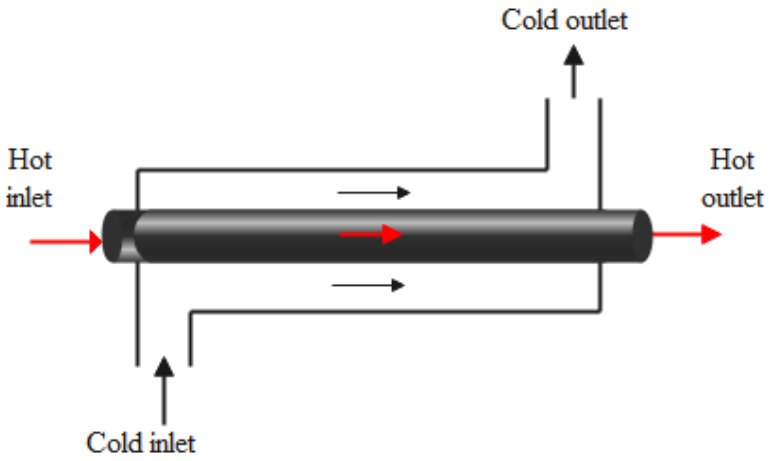

Figure 2. 3 Double pipe heat exchanger

Plate heat exchanger: A plate heat exchanger is made up of numerous thin metal plates that separate the two fluids. In such an HE device, the direction in which the two fluids flow is mostly the opposite, so that the heat transfer efficiency of the device is improved. A plate heat exchanger works by the principle that the heat of the hot fluid is connected to the wall of the plate, and then the plate wall conducts the heat energy to the other side. Finally, the heat energy will be taken away from the plate wall and transferred to the other fluid by convection (Lavine, 2017)(Khan, 2017).

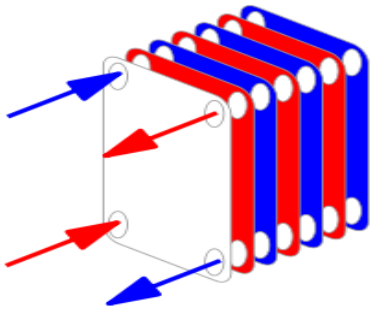

Figure 2. 4 Plate heat exchanger

Spiral heat exchanger: Spiral HE is made up of two concentric spiral channels. The concentric channels are made from a tube that is wrapped by two long, flat plates. In a spiral HE device, hot fluids enter and leave the first channel spirally, while cold fluids also flow spirally to the other side of the spiral channel. Spiral HE is most commonly used to transfer heat energy between viscous fluids (Lavine, 2017)(Khan, 2017).

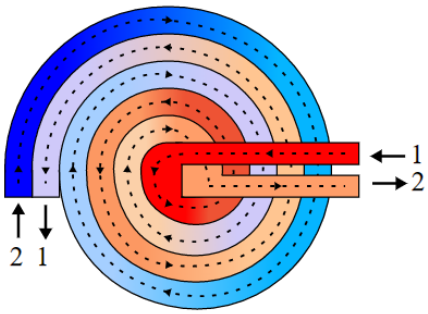

Figure 2. 5 Spiral heat exchanger

Shell and tube heat exchanger: A STHE is a thermal device that contains a collection (bundle) of tubes inside the shell. In such a HE device, the controlling fluid passes through the collection tube and the other fluid passes through the shell side. In such devices, the wall of the tube serves as a medium for the heat to be transferred between the two fluids. STHE is one of the most commonly used HE devices in process industries, chemical

industries, and other industries. This is due to their mechanical robustness and flexibility, and their ability to operate at various ranges of temperature and pressure. A typical structure of the STHE is shown in figure 2.6 (Dodd, 1983).

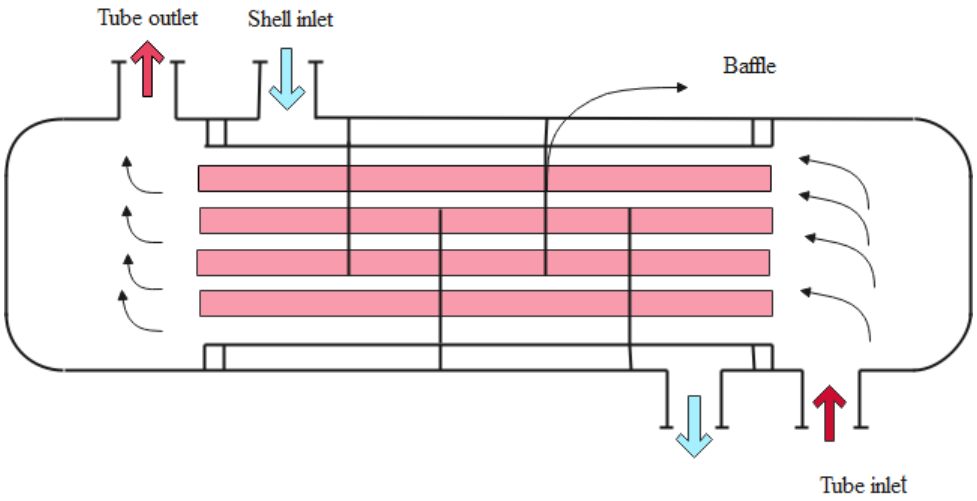

Figure 2. 6 Shell and tube heat exchanger

As can be observed in fig. 2.6, a STHE is made up of three main components, namely the baffle, the bundle of tubes, and the shell. The baffle assists the tube in such a way that the flow through it follows an approximately natural manner. From the above figure, we can observe that one fluid flows inside the tube, and the other flows within a shell (outside the tube).

2.2.3. Advantages of shell and tube heat exchanger over other type

STHEs are, without a doubt, the most common and widely used thermal devices in a variety of industries. The reasons that make them the choice in many industries are (Dodd, 1983) (Khames et al., 2020):

- They are fabricated widely
- They are designed with good thermal and mechanical design.
- They provide large surface areas for the heat to be transferred.
- They are designed in a variable range of sizes, from the smallest to the largest.
- They can be cleaned and maintained easily and are suitable for both mechanical and chemical cleaning purposes.

- Since they are mechanically robust, they are capable of resisting sensitivity to transportation and production, abnormal operating conditions, and fabrication stress.
- Since they have good mechanical and thermal design, the probability of their components being exposed to failure is less; even if failure has happened, they can be easily replaced.

All the above-mentioned advantages have made STHE the most powerful and reliable thermal device for most applications such as nuclear power plants, petrochemical, sewage treatment, food processing, beverage, chemical, pharmaceutical sectors, natural gas processing, etc.

2.3. Components of heat exchanger temperature control system

The components required to control the outlet temperature of STHE are the sensor, transmitter, controller, transducer, and control valve. The sensor detects the outlet temperature of the process variable and produces a proportional electrical signal. The detected signal is then converted to a standard electrical signal via the transmitter, which is in the range of 4–20 mA. Then the output of the transmitter unit is compared with the set point so that the error signal is sent to the controller unit. The controller generates an electrical signal that enters the transducer. Then the transducer converts the generated electrical signal to the pressure signal. Finally, the control valve adjusts the flow rate in proportion to the control signal (Coughanowr, Donald R, 2009).

2.3.1. Control valve

A control valve is the final control element that controls the flow of fluid by varying its opening and closing based on the signal it receives from the controller. This enables the control valve to control processes including temperature, level, pressure, and concentration, which are commonly controlled parameters in process industries. The actuator that positions the valve can be a pneumatic (air) actuator, electrical or hydraulic based on the needs of the industry. However, air (pneumatically) actuated control valves are the most commonly used types of actuators in process industries, and this is due to their reliability, fairly low price, simple design, and intrinsic safety (Seborg, 2017). Since an air-actuated control valve is considered in this thesis, its type and working principles will be discussed.

An air-actuated control valve uses the pressure of the air as a source of power to position the valve according to the command it is given from the controller. An air-actuated (pneumatic) control valve can either be air-to-open or air-to-close based on the response of the control valve to the pressurized air. In the air-to-close control valve type, the flow rate is inversely proportional to the pressure signal, which means the flow is restricted with the increase in pressure signal, whereas in the air-to-open control valve type, the flow rate of the fluid is directly proportional to the pressure signal. An air actuated control valve is shown in figure 2.7 (Coughanowr, Donald R, 2009).

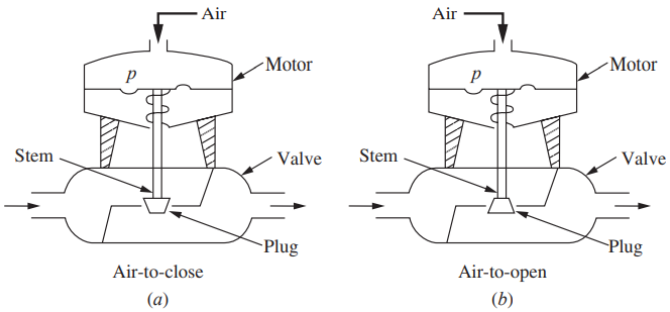

Figure 2. 7 Air actuated control valve (a) air to close; (b) air to open

As can be observed in figure 2.7, an air-actuated control valve is composed of an actuator, stem, valve body, plug, diaphragm, valve packing, and seat. The air-actuated control valve works based on the principle that the generated electrical signal from the controller is converted into a pressure signal by current to a pressure transducer. Once the pressure signal is generated, the actuator transfers mechanical power to the plug using the stem. Finally, the plug controls the flow by adjusting its opening and closing.

2.3.2. Temperature sensor

Sensors are considered as the eyes of process control that enable it to see the state of the process variable. “Indeed, one statement made about control is, if you can measure it, you can control it (Goodwin et al., 2000)”. Temperature sensor is a device that infers temperature deviation using a physical property that depends on temperature. The most frequently used temperature sensors are thermocouple, RTD, and thermistor.

Thermocouple temperature sensor: A thermocouple is a robust, simple, and cost-effective temperature sensing device, and it works based on the principle that two different metals with different electromotive forces (emf) are connected to each other at one end.

And since the connected two metals conduct heat differently, a temperature gradient will be created between them, which will allow them to measure the voltage difference between them (Morphet, 2017). Generally, a thermocouple measures a change in temperature of the process by measuring a voltage difference between the two connected metals. That means a thermocouple produces a voltage that depends on the temperature gradient (Seborg, 2017). Depending on the temperature ranges the thermocouple experiences, different types of wire are utilized. These wires are represented by different letters. The list of the letters and the ranges of the temperatures they cover are listed in (Morphet, 2017).

2.4 Related work

Authors in literature (Olana, 2021) have taken the STHE temperature control system as a case study to compare the performance of three tuning methods of PID, namely ZN Tuning, Chein et al., and the Cohen-Coon tuning method. From the obtained simulation result, it can be understood that when compared to the ZN tuning algorithm, Cohen-Coon has got better performance. The performance of the STHE control system is further improved when the PID is tuned using Chein et al. However, authors in this literature have only implemented the classical tuning method to compare the performances; no advanced control strategies have been compared. This thesis will compare the performance of the classical tuning method, advanced tuning method and an intelligent controller.

Authors in literature (Srivastava et al., 2016) have compared the performance of the fuzzy logic controller with that of the classical PID controller in terms of maximum overshoot and settling time. Consequently, the fuzzy logic controller provides much better performance. However, the fuzzy logic controller has a limitation in that it is not an expert by itself. It needs an expert to make it an expert and provide the best performance. Therefore, if the expert assigns the wrong rules, then the fuzzy logic controller may provide poor performance. This thesis integrates an artificial neural network with the fuzzy logic controller to make it an expert by itself. Then the performance of the ANFIS PD controller will be compared with that of the classical and GA-based PID controllers.

Authors in literature (Dizaji et al., 2015) have implemented a PID feed-forward controller to control the outlet temperature of the STHE system. The authors have demonstrated the system's response using MATHLAB and Simulink. But while developing the Simulink model, the author doesn’t consider the disturbance due to temperature variation of the input

fluid, which has an impact on the system's performance. Among the proposed controllers in this thesis, the ANFIS PD has provided the best performance despite the presence of disturbance effects.

Authors in literature (Tuntas, 2019) compared the performance of the ANN method to that of a traditional PID controller. The performance measures that the authors used to compare the two controllers are maximum overshoot and settling time. Thus, the simulation result has shown that the ANN has improved performance in both settling time and maximum overshoot. However, the result has taken a long time to settle, which is undesirable. Among the proposed controllers in this thesis, the ANFIS has got much better performance than the mentioned controllers in the literature.

Authors in literature (Somasundar Reddy & Balaji, 2020) have designed a G_A optimized PID controller to evaluate the performance of a shell and tube heat exchanger in terms of transient response. The result has shown that the GA optimized PID controller has improved the performance of the exchanger in terms of settling time, but the result has certain overshoot. Moreover, while simulating the system, the authors don't consider the time delay, even though the process exhibits a certain amount of delay. This delay has an impact on system performance. In this thesis the performance is evaluated with the presence of time delay effect.

Authors in literature (G. M. Sarabeevi and M. L. Beebi, 2016) have designed and compared the performance of internal model-based PID, internal model controller, and feed-forward plus internal model-based PID controller. The performance of the three controllers was investigated with and without the presence of disturbance. Their performance has been compared based on transient response and error-based criteria. The simulation results have shown that the performance of the feed-forward plus internal model-based PID controller provides better performance when compared to the other two controllers. However, the designed feed forward plus internal model-based PID controller follows a model-based strategy to calculate optimal control action, and most models of a process are accompanied by model uncertainty. Moreover, the designed controller has taken a longer time to settle. Among the proposed controllers through this thesis, the ANFIS provided better performance in terms of settling time and maximum overshoot than the controllers mentioned in the literature.

Authors in literature (Reddy & Balaji, 2021) have designed a fuzzy PID controller for STHE. While designing a controller, the author has also added a feed forward controller so that the performance of the system will not be reduced as a result of the flow variation of the input fluid, which significantly affects system performance. And then they compared the performance of the two controllers in terms of dynamic response characteristics such as settling time and maximum overshoot. The simulation result indicates that the proposed fuzzy-PID in conjunction with feed forward provides the best performance. However, from the simulation result, it can be observed that the performance of the system still needs an improvement so that the settling time will be as short as possible and the maximum overshoot is minimized. Among the proposed controllers in this thesis, ANFIS PD has provided better maximum overshoot and settling time than the mentioned literature.

The reviewed literature reveals that the design of an effective controller for STHE is a difficult task. This is because of the non-linearity, complexity, uncertainty, time delay effect and presence disturbance. The other thing that can be understood from the reviewed literature is the existence of a trade-off between transient response and steady state response to a STHE temperature control system. A controller that has a good transient response may result in poor steady state performance.

CHAPTER THREE

3. METHODOLOGY AND SYSTEM MODELING

This chapter comprises the methodologies that have been adopted throughout this thesis. The characteristics and properties of the material and software used are explained. Moreover, the dynamic model of the proposed system has been modeled so as to give the physical incite of the proposed system. Finally, the system specifications have been assigned from a closely related paper.

3.1. Materials

The materials that have been used in this thesis include software such as Microsoft Office 2016, MATLAB/2019a, Wonder Share edrawMax, MathType6.0, and Mendeley reference manager. Microsoft Office has been used for writing and editing the thesis document. MathType has been used for developing mathematical formulas and equations in Microsoft Office Word and PowerPoint as well. MATLAB is used to develop a Simulink model as well as write MATLAB codes. Wondershare edrawMax has been used to draw pictures, flowcharts, and block diagrams. For citation and reference purposes, Mendeley reference manager has been used.

3.2. Methods

The methods that have been followed to meet the general and specific objectives mentioned in chapter one are summarized in the flow chart shown in figure 3.1. First, related works from journals and articles are reviewed. Then each and every component of the proposed systems is modeled dynamically from the conservation law of energy (first law of thermodynamics) and other laws. Then the parameters have been assigned to the modeled system from the experiment performed in closely related work, and the proposed controllers have been implemented into the STHE control system. Finally, the simulation results of the proposed controllers have been compared and analyzed.

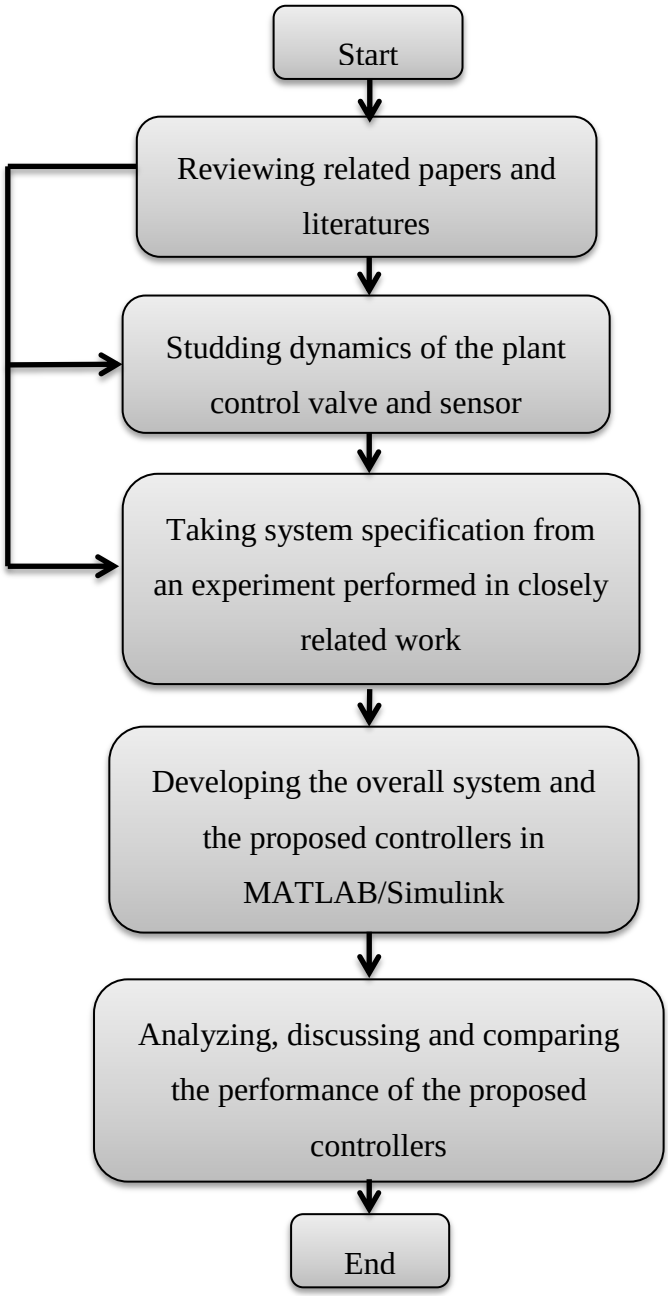

Figure 3. 1 Flow chart of the research methodology

3.3. Schematic and block diagram of the proposed system

3.3.1. Schematic diagram of the proposed system

The schematic diagram of the proposed STHE temperature control is shown in figure 3.2. As can be observed on the schematic diagram, two fluids are being supplied to the system. Superheated steam is supplied from the boiler to the tube side, and process fluid is supplied from the storage tank to the shell side of the STHE.

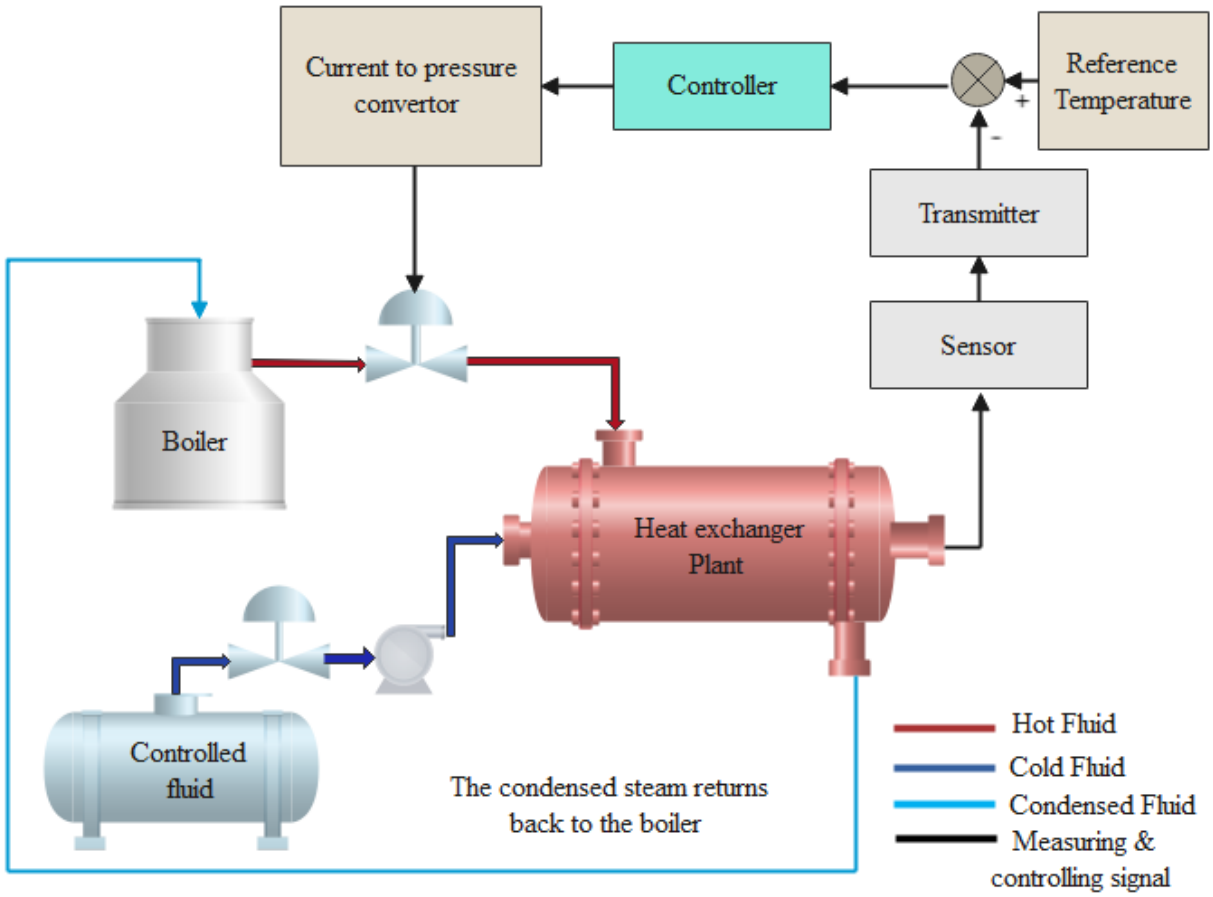

Figure 3. 2 Schematic diagram of the proposed system (Padhee et al., 2011)

Here, the main objective is to regulate and sustain the temperature of the process fluid at the desired set point (reference temperature) by varying the flow rate of the steam, and this is achieved based on the following principle: the outlet temperature of the process fluid that is measured by the thermocouple temperature sensor is compared with the desired temperature. The deviation between the two is calculated, which is going to be fed as an input to the proposed controller. Since the signal generated by the controller is a current signal, it is converted to a pressure signal via a current to pressure converter. Finally, this pressure signal positions the valve in proportion to the control signal.

3.3.2. Block diagram of the proposed system

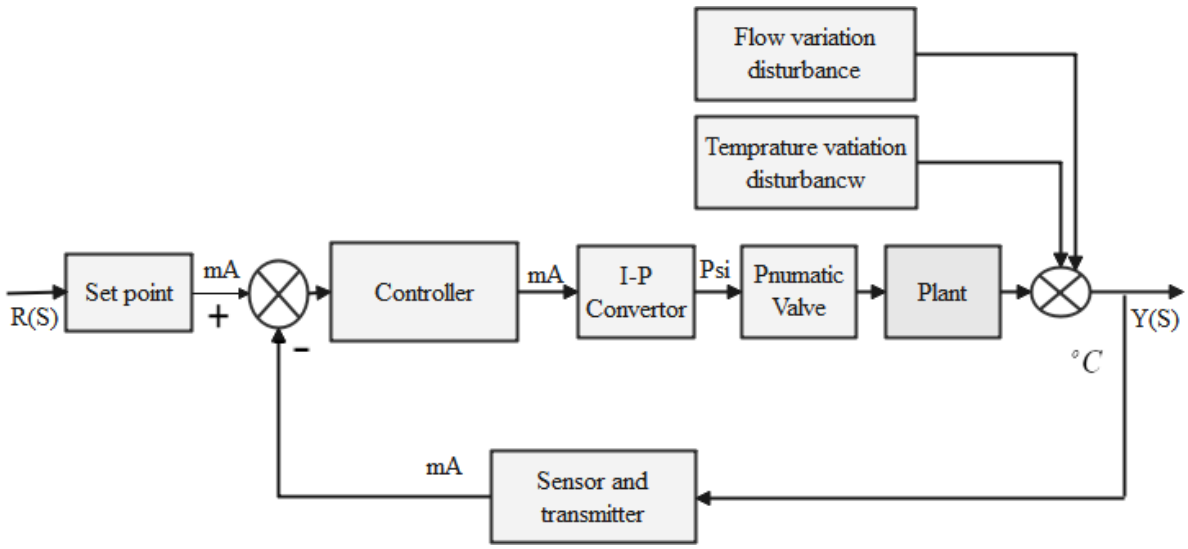

Figure 3. 3 Block diagram of the proposed system (Padhee et al., 2011)

From the block diagram shown in figure 3.3, it can be clearly observed that the proposed system is subjected to the flow variation of the input fluid and the temperature variation of the input fluid disturbance effect.

3.4. Dynamics of a shell and tube heat exchanger control system.

3.4.1 Plant dynamics

The dynamic model of the HE plant is modeled from the energy balance equation of thermodynamics. The first law of thermodynamics can be represented as (Coughanowr, Donald R, 2009):

$$\begin{Bmatrix}\text{Rate of energy}\\ \text{accumulation}\end{Bmatrix} = \begin{Bmatrix}\text{Rate of energy in}\\ \text{by convection}\end{Bmatrix} - \begin{Bmatrix}\text{Rate of energy out}\\ \text{by convection}\end{Bmatrix} + \begin{Bmatrix}\text{Net rate of heat energy added}\\ \text{from steam heater}\end{Bmatrix} + \begin{Bmatrix}\text{Total work done on the system}\\ \text{by the surrounding}\end{Bmatrix} \quad (3.1)$$

For the heat exchanger system, accumulated energy is taken as internal energy, and energy due to the total work done by the environment is negligible when it is compared to energy

by convection and the heat transferred from the steam heater. Consequently, the balanced energy on the heat exchanger can be represented as (Seborg, 2017):

$$dU_{\text{int}} = U_I - U_O + q \tag{3.2}$$

Where U_{int} is internal energy (J), U_I inflow energy rate by convection (J), U_O is outflow energy rate by convection (J), q is net energy added from the steam heater (J).

The dynamic model of the plant is developed based on the following assumptions: (Coughanowr, Donald R, 2009)(Seborg, 2017)

- ✓ The inlet flow and outlet flow rates of the exchanger plant are equal so that the level (volume) of the fluid in the plant is maintained constant.
- ✓ The density and the heat capacity of the liquid are assumed to be constant so that their temperature dependence is negligible.
- ✓ The heat storage capacity of the insulating wall is negligible, and the heat loss is also assumed to be negligible.

The inlet and outlet energy by convection for equation (3.2) is expressed in terms of mass or volumetric flow rate as follows (Seborg, 2017):

$$U_I = M_r \overline{H}_i = V_r D \overline{H}_i \tag{3.3}$$

$$U_o = M_r \overline{H} = V_r D \overline{H} \tag{3.4}$$

By substituting the equations (3.3) and (3.4) into the equation (3.2), the internal energy equation becomes:

$$dU_{\text{int}} = M_r \overline{H}_i - M_r \overline{H} + q \tag{3.5}$$

Where U_{int} is internal energy (J), M_r is mass flow rate (Kg/s) $\overline{H}_i$ is inlet enthalpy per unit mass (J / Kgs^{-1}) $\overline{H}$ is outlet enthalpy per unit mass (J / Kgs^{-1}). For liquids, the internal energy is approximately equal to the enthalpy. Therefore, we can represent the internal energy and internal energy per unit mass as follows (Seborg, 2017):

$$U_{\text{int}} \approx H \tag{3.6}$$

$$\overline{U}_{\text{int}} \approx \overline{H} \tag{3.7}$$

$\overline{H}$ is a pressure and temperature dependent parameter, it is expressed as a function of pressure and temperature as shown below (Seborg, 2017).

$$\overline{H} = \overline{H}(P,T) \tag{3.8}$$

For differential change in temperature (T) and pressure (P) $\overline{H}$ is expressed as:

$$. d\overline{H} = \left(\frac{\partial \overline{H}}{\partial T}\right)_P dT + \left(\frac{\partial \overline{H}}{\partial P}\right)_T dP \tag{3.9}$$

Heat capacity is defined as the rate of change of enthalpies per unit mass at constant pressure (Seborg, 2017).

$$C_P \triangleq \left(\frac{\partial \overline{H}}{\partial T}\right)_P \tag{3.10}$$

Substituting (3.10) in (3.9) we will obtain

$$d\overline{H} = C_P dT + \left(\frac{\partial \overline{H}}{\partial P}\right)_T dP \tag{3.11}$$

For liquids $\left(\frac{\partial \overline{H}}{\partial P}\right)_T \approx 0$ (Seborg, 2017). Then the differential change of equation (3.11) can be represented as:

$$d\overline{H} = C_P dT \tag{3.12}$$

Consequently, the differential change in enthalpy per unit mass is expressed as:

$$\frac{d\overline{U}_{\text{int}}}{dt} = \frac{d\overline{H}}{dt} = C_P dT \tag{3.13}$$

Systems' accumulated (total) enthalpy can be represent in terms of enthalpy per unit mass or volume (Sarabeevi, G. M., 2016).

$$U_{\text{int}} = DV\overline{U}_{\text{int}} \tag{3.14}$$

Where V is a volume (m^3) and D is the density (Kg/m^3) of the liquid respectively.

Then the differential change of the total internal energy will be represented as:

$$\frac{dU_{\text{int}}}{dt} = \frac{d(DV\overline{U}_{\text{int}})}{dt} = DV\frac{d\overline{U}_{\text{int}}}{dt} \qquad (`3.15)$$

By Substituting (3.13) in (3.15) the differential of total internal energy is given as:

$$\frac{dU_{\text{int}}}{dt} = DV\frac{d(\overline{U}_{\text{int}})}{dt} = DVC_P\frac{dT}{dt} \qquad (3.16)$$

Where C_P is heat capacity the fluid at constant volume ($J/Kg\,^oC^{-1}$), $T_i(t)$ is inlet temperature, (^oC) and $T(t)$ is outlet temperature ^oC.

Now we have derived an equation for the left side of equation (3.2), let us drive the expression for the right side enthalpy term of equation (3.2). Suppose the controlled liquid in the plant (shell) is at temperature T, integrating the per unit mass enthalpy term from the reference temperature to T we will have:

$$\frac{d\overline{H}}{dt} = C_P dT \qquad (3.17)$$

$$\overline{H} = C_P\int_{T_R}^{T} dT = C_P(T - T_R) \qquad (3.18)$$

Similarly for inlet fluid

$$\overline{H}_i = C_P\int_{T_R}^{T} dT = C_P(T_i - T_R) \qquad (3.19)$$

Substituting (3.16), (3.18) and (3.19) in (3.2) we will have:

$$DVC_P\frac{dT}{dt} = M_rC_P(T_i - T_R) - M_rC_P(T - T_R) + q \qquad (3.20)$$

For steady-state conditions, the equation (3.20) will become (Coughanowr, Donald R, 2009):

$$DVC_p\frac{dT_s}{dt} = M_rC_P(T_{is} - T_{Rs}) - M_rC_P(T_s - T_{Rs}) + q_s \qquad (3.21)$$

The subscript "s" is used to indicate a steady-state condition of the system. Subtracting (3.21) from (3.20), and then canceling like terms and rearranging it, we will obtain:

$$M_rC_P(T_i - T_{is}) - M_rC_P(T - T_s) + q - q_s = DVC_p\frac{d(T - T_s)}{dt} \qquad (3.22)$$

In this thesis, temperature variation of the input fluid is taken as a disturbance, so while modeling the dynamics of the system; the input temperature is assumed to be constant. Then, by introducing the deviation variables of (3.23) and (3.24), we will obtain the first-order differential equation shown by equation (3.25).

$$T' = T - T_s \tag{3.23}$$

$$Q = q - q_s \tag{3.24}$$

$$DVC_P \frac{dT'}{dt} = -M_r C_P T' + Q \tag{3.25}$$

In s domain (3.25) can be written as

$$DVC_P T'(s)s = -M_r C_P T'(s) + Q(s) \tag{3.26}$$

Rearranging equation (3.26) we will obtain the equation shown below:

$$\frac{DV}{M_r} sT'(s) = -T'(s) + \frac{1}{M_r C_P} Q(s)$$

$$\text{Let } K_P = \frac{1}{DVC_P} \text{ and } \tau_P = \frac{DV}{M_r}$$

After collecting like terms and rearranging (3.26), the transfer function will be obtained as:

$$G_P(s) = \frac{T'(s)}{Q(S)} = \frac{K_P}{(\tau_P s + 1)} \tag{3.27}$$

Transportation lags (time delay)

A temperature change was supposed to be measured directly from the outlet side of the plant, but practically, this device is not directly connected to the outlet stream of the plant (Sarabeevi, G. M., 2016). This is done to protect the sensor from damage; therefore, it is located in the downstream pipeline of the plant**.** In this situation, the measured temperature encounters some amount of delay. This delay is the time required for the fluid to travel from point A to point B in figure 3.4. Time delay is sometimes called dead time or transportation lag.

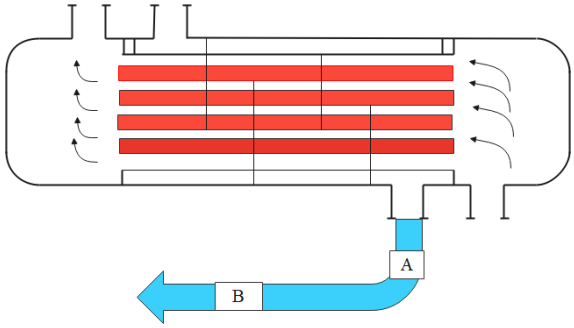

Figure 3. 4 Sensor position

From figure 3.4, we can observe that there is a delay while sensing a temperature. Let the actual temperature at point A be T' and the measured temperature at point B be T_1'. Then T_1' becomes the delayed version of T'.

$$T_1'(t) = T'(t - \tau_d) \tag{3.28}$$

$$\tau_d = \frac{Volume \text{ of tube}}{volumetric \text{ flow rate}} \tag{3.29}$$

Taking the Laplace transformation of equation (3.28) we will obtain

$$T_1'(s) = e^{-s\tau_d} T'(s) \tag{3.30}$$

$$\frac{T_1'(s)}{T'(s)} = e^{-s\tau_d} \tag{3.31}$$

Then the transfer function of the process with the presence of time delay is represented as:

$$G_P(s) = \frac{K_P e^{-s\tau_d}}{\tau_P s + 1} \tag{3.32}$$

3.4.2. Control valve dynamics

The size of the opening and closing of the control valve is determined by the position of the plug. The plug is positioned in proportion to the force received from the pneumatically actuated actuator on the diaphragm of the control valve. The balanced force acting on the plug is determined as (Sharma et al., 2011):

$$P_d A = Kx + C\frac{dx}{dt} \tag{3.33}$$

Where $P_D A$ is a force exerted at the top of the diaphragm by compressed air, Kx is a spring force that occurs due to the attached spring between the diaphragm and stem, and Cdx/dt is an upward frictional force that results from the close contact of the valve packing with the stem. Taking the Laplace transformation for both sides of the equation (3.33), we obtain:

$$AP_d(s) = Kx(s) + Csx(s) \tag{3.34}$$

Where A is area of the diaphragm (m^2), K is hooks constant (N/m), P_D is exerted pressure on the diaphragm (Psi), x is the displacement (m). After rearranging (3.34) the equation shown below will be obtained

$$G_V = \frac{x(s)}{P_d(s)} = \frac{A/K}{(c/k)s+1} \tag{3.35}$$

Let A/K be K_V and c/k be τ_V then the transfer function of the control valve is represented by the first order TF.

$$G_V = \frac{x(s)}{P_d(s)} = \frac{K_V}{\tau_V s+1} \tag{3.36}$$

Current-pressure convertor gain: As explained in the review part of this thesis, the electrical signal generated from the controller has to be converted to the pressure signal so that the pneumatically actuated control valve understands the signal generated from the controller. This is done with the help of current-pressure converter gain. This gain is the ratio of valve capacity to the pressure range as shown in the equation below.

$$I-P \text{ converter} = \frac{\text{pressure range}}{\text{Temperature range}} \tag{3.37}$$

3.4.3. Sensor and transmitter dynamics

As explained in the review section of this thesis, the thermocouple temperature sensor produces a mV signal that increases or decreases as temperature increases or decreases, respectively. The produced output signal of a temperature sensor is not compatible with the input range of the controller (Seborg, 2017). To achieve compatibility of the sensor with the controller, the transmitter is integrated with the sensors. The first-order differential equation of the sensor and transmitter is represented as (Sarabeevi, G. M., 2016):

$$\tau_s \frac{dI(t)}{dt} + I(t) = K_m T(t) \tag{3.38}$$

Taking Laplace transformation

$$\tau_s sI(s) + I(s) = K_m T(S) \Rightarrow I(s)(\tau_s s + 1) = K_m T(S) \tag{3.39}$$

Rearranging (3.39)

$$G_S(S) = \frac{I(s)}{T(S)} = \frac{K_m}{\tau_s s + 1} \tag{3.40}$$

Transmitter gain: is represented by the slope between the transmitter's output range and the adjusted input range of the sensor. The industrial standard transmitter range is 4mA-20mA or 0-5v in terms of current and voltage, respectively. But the most commonly integrated transmitter is in the current range.

$$K_m = \frac{\text{transmitter's output range}}{\textit{sensors} \text{ input range}} \tag{3.41}$$

Table 3. 1 STHE control system parameter specification (Hanke, 2007)(Padhee et al., 2011)

Parameter	Value[unit]
Exchanger response to steam flow gain	50 [^{o}c / (Kg / sec)]
Exchanger time constant	30 [sec]
Exchanger response to flow variation gain	1 [^{o}c / (Kg / sec)]
Exchangers response to Temperature variation gain	3 ^{o}c / ^{o}c
Control valve capacity	1.6 [Kg/sec]
Time constant of the control valve	3 [sec]
Temperature sensor range	(50 to 150) [^{o}c]
Temperature sensors time constant	10 [sec]

By substituting the above specifications, the transfer function of the process, control valve sensor, current to pressure transducer gain, and transmitter gain are obtained as:

$$G_p = \frac{50e^{-\tau_d s}}{30s+1} \tag{3.42}$$

$$K_V = \frac{1.5Kg/s}{(15-3)psi} = 0.13Kg/s(psi) \tag{3.43}$$

$$G_V = \frac{0.13}{3s+1} \tag{3.44}$$

$$I-P \text{ converter} = \frac{(15-3)\text{ Psi}}{(20-4)\text{ mA}} = 0.75 \text{ Psi/mA} \tag{3.45}$$

Where G_p transfer function of the plant is, K_V is control valve gain, G_V is control valve transfer function. The overall transfer function of the plant with the control valve is represented by SOPDT as shown in equation 3.46:

$$G(s) = \frac{4.875e^{-\tau_d s}}{90s^2+33s+1} \tag{3.46}$$

$$K_m = \frac{(20-4)mA}{(150-50)^o c} = 0.16mA/^o c \tag{3.47}$$

$$G_S(s) = \frac{0.16}{10s+1} \tag{3.48}$$

$$G_{dF}(s) = \frac{1}{30s+1} \tag{3.49}$$

$$G_{dT}(s) = \frac{3}{30s+1} \tag{3.50}$$

Where K_m, is transmitter gain G_s, is transfer function of the sensor G_{dF}, flow disturbance transfer function G_{dT} is temperature disturbance transfer function.

CHAPTER FOUR

4. CONTROLLER DESIGN

4.1. PID controller

Around 90% of the control loops in the process industry are PID control loops (Abdullah, 2019). This is due to its simplicity, cost-effectiveness, and ease of implementation (Valarmathi, 2018). The PID controller may have either a parallel or serious arrangement. The parallel arrangement is shown in figure 4.1. In a PID controller, the proportional term generates a control signal which is proportional to the error signal boost the response, whereas the derivative term improves the transient response (stability) and the integral term eliminates steady-state error (Meena, 2017).

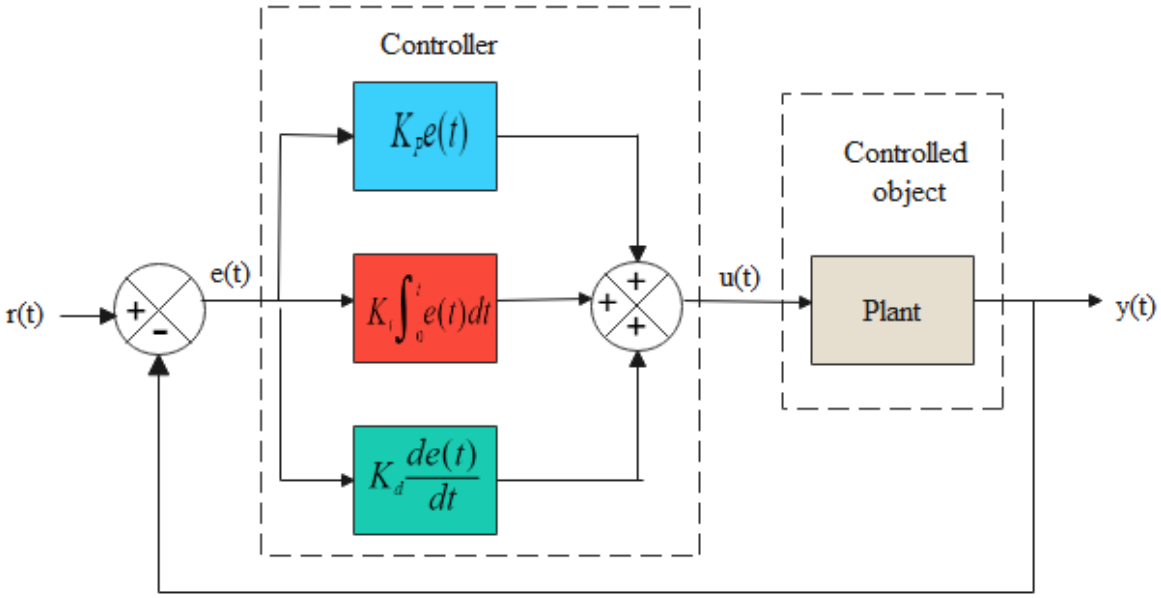

Figure 4. 1 Structure of PID controller (Manipatruni, 2018)

Where K_p is the proportional gain, K_i is integral gain, K_d is derivative gain r (t) is set point, e (t) is the error signal, and y (t) is the output of the controlled system. The error signal e (t) is the deviation between the actual output and the desired output by the process (set point). The time domain representation for the parallel PID controller structure are shown in equation (4.1) (Eldin & Awouda, 2017)(Gani et al., 2019).

$$U(t) = \underbrace{K_P e(t)}_{\text{Proportional action}} + \underbrace{K_i \int e(t)dt}_{\text{Integral action}} + \underbrace{K_d \frac{de(t)}{dt}}_{\text{Derivative action}} \quad (4.1)$$

Table 4. 1 Table Effect of PID gains on steady and transient state performance

Gain	Overshoot	Settling time	Steady state error
Proportional	Increase	Small change	Decrease
Integral	Increase	Increase	Decrease
Derivative	Decrease	Decrease	No change

4.1.1 Ziegler-Nichols tuning method

The ZN tuning method is the most commonly used classical tuning method. In such a tuning method, the gains of PID are tuned by either by finding the dead time and time constant or finding the critical gain and critical time period. In this thesis, the latter has been chosen. The critical gain and time period are calculated by applying Routh stability criteria to the proposed system's characteristic equation (Reddy & Balaji, 2021). The classical PID controller is a linear system control method; therefore, the linear plant model is taken. Then the linear feed-back loop of the proposed system is presented in figure 4.2.

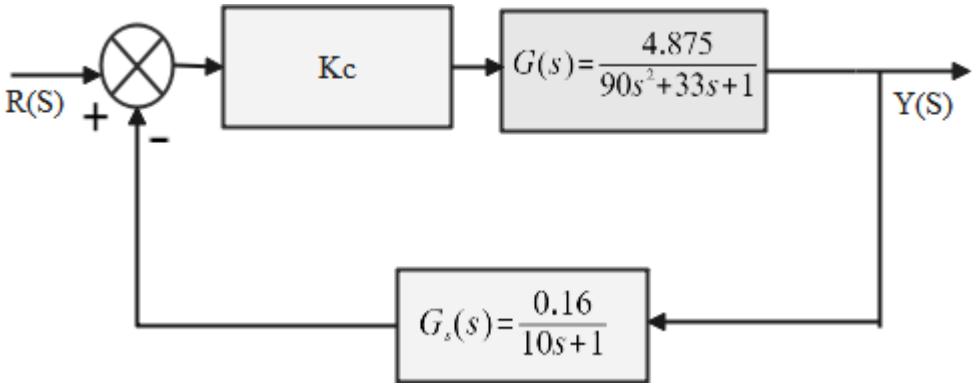

Figure 4. 2 Feed-back loop of the proposed system

The closed loop transfer function of the proposed system is then obtained as:

$$\frac{Y(s)}{R(s)} = \frac{Kc * G(s)}{1 + Kc * G(s) * G_s(s)} \quad (4.2)$$

From equation (4.2) the characteristic equation of the proposed system is:

$$1+Kc*G(s)*G_s(s)=1+\frac{0.78Kc}{900s^3+420s^2+43s+1} \tag{4.3}$$

$$1+Kc*G(s)*G_s(s)=\frac{900s^3+420s^2+43s+0.78Kc+1}{900s^3+420s^2+43s+1} \tag{4.4}$$

Based on the ZN tuning algorithm, the critical gain is found by equating the characteristic equation to zero(Hanke, 2007).

$$\frac{900s^3+420s^2+43s+0.78Kc+1}{900s^3+420s^2+43s+1}=0 \tag{3.5}$$

$$900s^3+420s^2+43s+0.78Kc+1=0 \tag{4.6}$$

The necessary and sufficient condition for Routh stability criteria is that each turn of the first column of the Routh array must be positive. If this condition is not satisfied, the system is unstable and the number of signs changed in the first column corresponds to the number of roots of the characteristic equation in the right half of the 'S' plane (Hanke, 2007). The Routh array is represented as follows:

s^3	900	43
s^2	420	0.78Kc+1
s^1	$\frac{420*43-900*(0.78Kc+1)}{420}$	0
s^0		

By applying Routh stability criteria to the above array, the equation below is found:

$$\frac{420*43-900*(0.78Kc+1)}{420}\geq 0 \tag{4.7}$$

$$420*43-900*(0.78Kc+1)\geq 0 \tag{4.8}$$

Rearranging equation (4.8), the critical gain is found to be Kc $\leq$23.8. Using the equality, Kc = 23.8.

Once the critical gain is calculated, the critical frequency is calculated by representing equation (4.6) in jw form. Substituting the value of Kc, the equation shown below is obtained.

$$900(jw)^3 + 420(jw)^2 + 43(jw) + 0.78 * 23.8 + 1 = 0 \tag{4.9}$$

$$-900\,jw^3 - 420w^2 + 43\,jw + 19.6 = 0 \tag{4.10}$$

Equating the real part to zero, the critical frequency is obtained to be 0.218. Then the critical time period is then calculated by using the formula shown below.

$$T = \frac{2\pi}{w} = \frac{2 * 3.14}{0.218} = 28.79 \tag{4.11}$$

Once the critical gain and time period are obtained, the parameters of the PID gains are adjusted as per the table shown below.

Table 4. 2 Ziegler-Nichols frequency response tuning criteria (Hanke, 2007)

Controller	Kp	Ti	Td
P	$0.5\,K_{cu}$		
PI	$0.45\,K_{cu}$	$T_c/1.2$	
PID	$0.6\,K_{cu}$	$0.5\,T_c$	$T_c/8$

Once the proportional gain, the integral time constant and the derivative time constant have been found the PID controller is represented by the equation below.

$$PID(t) = Kp\left(e(t) + \frac{1}{Ti(t)} + Td\,\frac{de(t)}{dt}\right) \tag{4.12}$$

The initial parameters obtained based on the above parameter setting may not provide satisfactory performance; therefore, it has to be repeatedly retuned based on minimizing the predefined objective function through trial and error in MATLAB. In this thesis, the parameters have been tuned based on minimizing the IAE objective function.

4.1.2. Genetic algorithm

GA is a search and optimization method that generates the best solution to a particular problem. This algorithm is inspired by evolutionary biology principles such as selection, crossover, mutation, and inheritance. Evolution in GA passes through four main stages, namely, initialization, selection, genetic operation, and termination (Ahmmed et al., 2020). In the initialization stage, evolution starts with randomly generated individuals from a given population. Then, from the initialized population, certain individuals are chosen

based on their fitness (defined by the assigned objective function). In the genetic operation stage, the chosen solutions are evolved so that the best solution is generated; the genetic operations performed are mutation and crossover. Finally, the algorithm terminates either when the maximum generation has been reached or a satisfactory solution has been obtained. If the result termination is due to exceeding the maximum generation, the obtained result may not be satisfactory. Through this thesis, the fitness evaluation functions that have been used as objective functions are ISE, IAE, and ITAE. These functions are also known as performance indices. The overall flow chart of GA optimization is shown in figure 4.3.

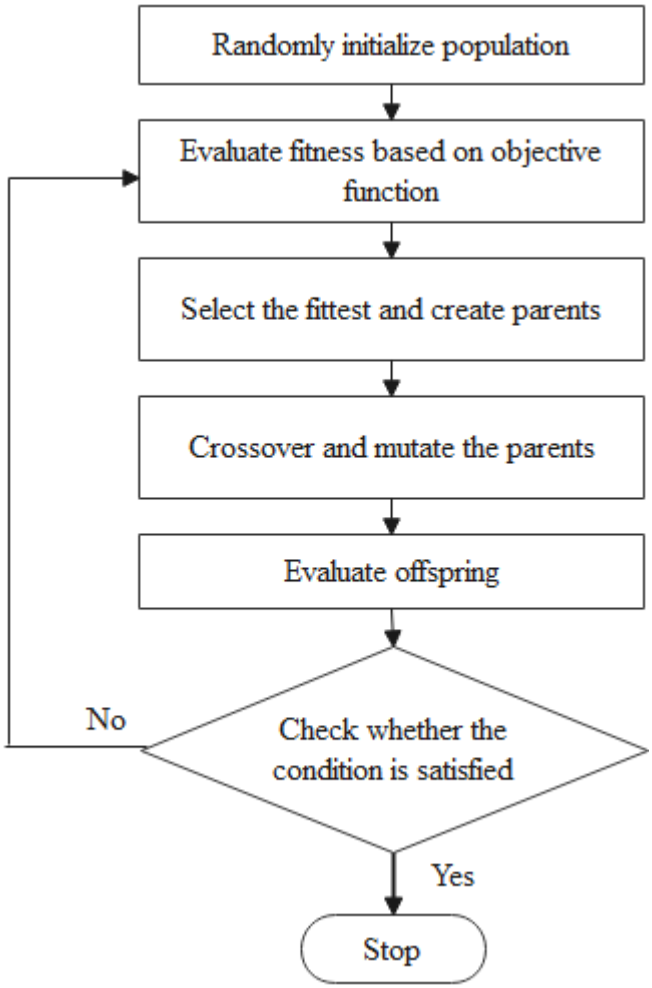

Figure 4. 3 Flow chart of GA algorithm (Tidke, 2018)

4.1.3. Performance indices

The overall performance of a control system is evaluated using different performance indices. The most common performance indices are integral square error (ISE), integral

absolute error (IAE), and integral time absolute error (ITAE). The equations for these performance indices are represented below (Suthar, 2017).

$$\begin{cases} IAE = \int_0^\infty |e(t)|\,dt \\ ITAE = \int_0^\infty t\,|e(t)|\,dt \\ ISE = \int_0^\infty e^2(t)dt \end{cases} \tag{4.13}$$

The GA parameters that have been set to obtain the optimal values of the PID gains are presented in table 4.3.

Table 4. 3 GA optimization parameter setting for PID controller

Parameter	Value
Population size	60
Maximum generation	90
Encoding	Binary
Selection	Uniform
Cross over	Single point
Mutation	Uniform
Number of parameter	3
Lower bound	[0 0 0]
Upper bound	[10 1 52]

Based on the above parameter setting, the unit step fitness curve of ISE, IAE, and ITAE objective functions is shown in figures 4.4, 4.5, and 4.6, respectively.

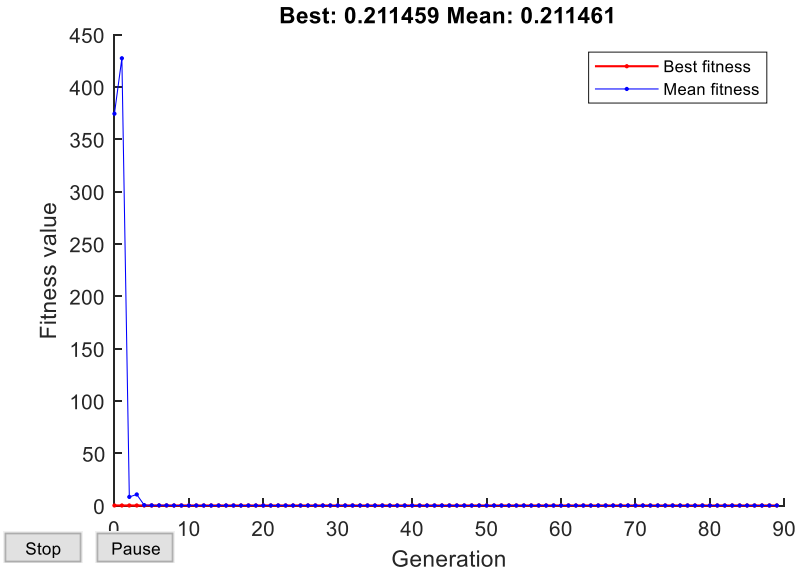

Figure 4. 4 Fitness value vs generation of ISE

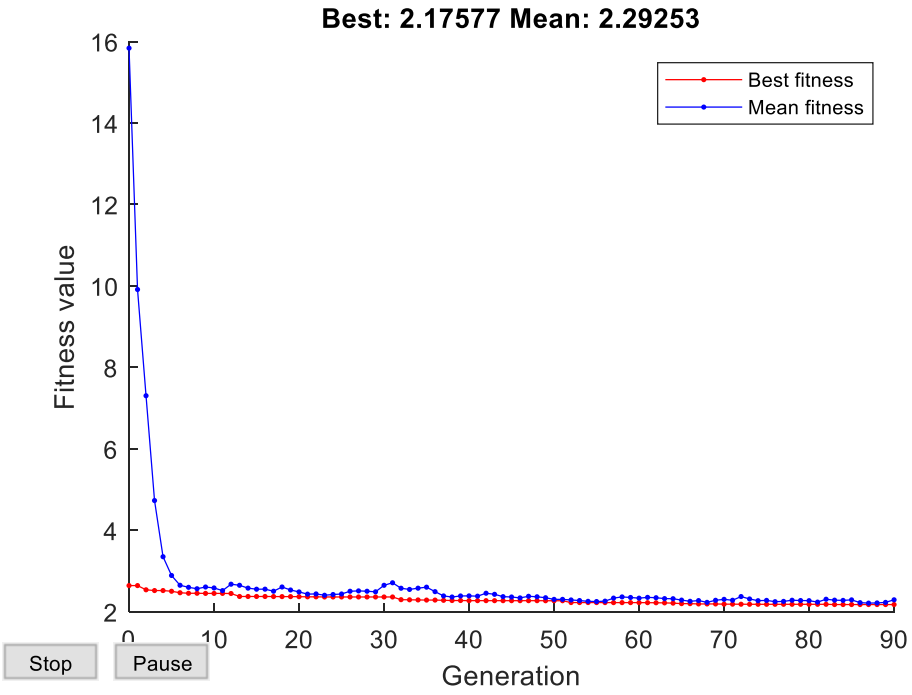

Figure 4. 5 Fitness value vs generation of IAE

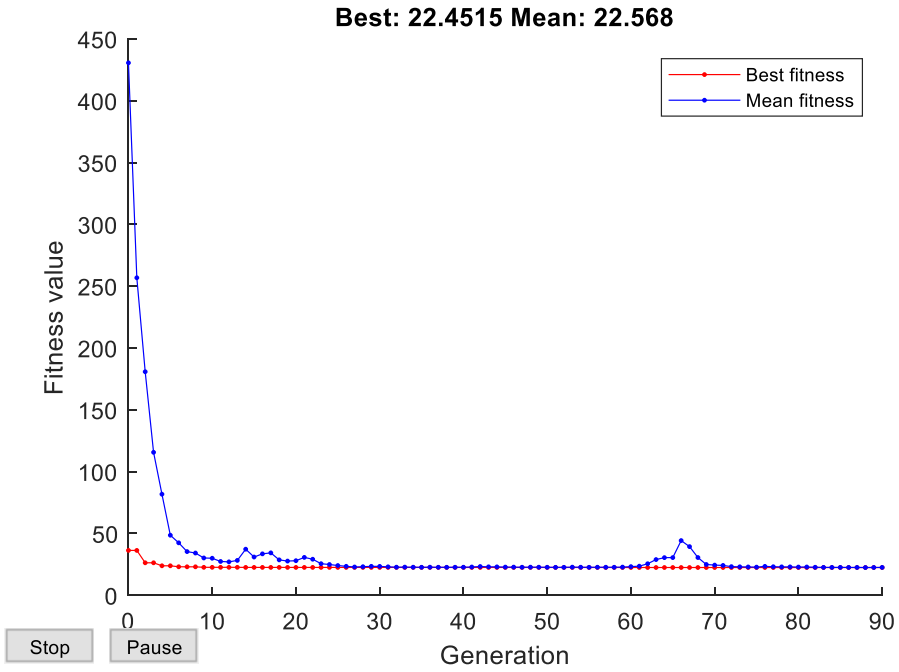

Figure 4. 6 Figure Fitness value vs generation of ITAE

4.2. Intelligent controller

The design of an intelligent system is inspired by the intelligence of human beings. The main objective of an intelligent control strategy is to integrate the intelligence of a human being into a control strategy. Such features include learning, adaptation, and reasoning. Intelligent controllers have been increasingly used in process industries such as biochemical, chemical, and biomedical engineering over the last three decades (Dutta & Upreti, 2021).

4.2.1. Fuzzy logic overview

The basic concept behind fuzzy logic is to extend the traditional crisp logic membership of an element to a given set. In crisp logic, an element either belongs or does not belong to a set, and consequently, its membership value is either 1 or 0, whereas in fuzzy logic, the membership function can have a value within the range of [0, 1] (García-Martínez et al., 2020) (Chen & Chang, 2018).

FLC converts the knowledge of an expert into an automatic control algorithm. Additionally, it has the capability to handle approximated information systematically. This makes it suitable for controlling nonlinear systems. If the assigned rule bases are effective,

the skilled human operator can be replaced by an FLC. In FLC design, both the input and output variables are crisp. And based on the way in which crisp output is generated, fuzzy inference mechanisms can be classified as mandani and sugeno. The former generates the crisp output through the defuzzification process, whereas the latter generates the crisp output by weighted average (Farah et al., 2018). The structure of FL is shown in figure 4.7.

The main difference between the Sugeno and Mandani inference mechanisms lies in the way crisp output is generated. In Mandani FIS, a defuzzification process is required, where as in Sugeno, the crisp output is obtained by weighted average. Another distinction between Mandani and Sugeno is that the consequent rules in Mandani are fuzzy, and thus the outputs in Mandani are expressed in terms of membership function, whereas the outputs in Sugeno are not expressed in terms of membership function. The inference mechanism used by the ANFIS algorithm is the Sugeno FIS (Liu et al., 2017).

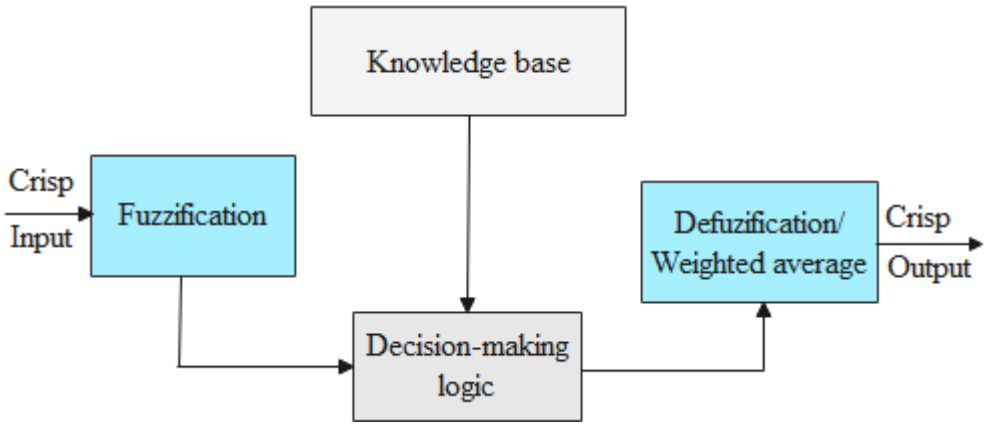

Figure 4. 7 Structure of FL (Eldin & Awouda, 2017)

As can be observed in figure 4.7, the inputs to the FLC and the output of fuzzy controllers are crisp**.** Hence, the first stage in the design of FLC is converting the crisp values to fuzzy values by a process of fuzzification. Then the knowledge-based decision making logic is constructed. Finally, the crisp output is generated by either defuzzification or weighted average (Liu et al., 2017). The different mechanisms of defuzzification used in the Mandani inference system are explained in (Mathworks, 2020).

Advantage of sugeno inference mechanism over mandani:

- ✓ Sugeno is computationally efficient.
- ✓ It works well with adaptation and optimization algorithms.
- ✓ Sugeno takes less processing time because the time taken to generate crisp output is weighted average.
- ✓ It doesn't possess a high computational burden because no custom defuzzification process is required.

Even though a FLC has the capability of achieving controllability and robustness by dealing with non-linearity and uncertainty, it has a limitation in that if an expert assigns a wrong rule, the performance is greatly distorted and might even be lower than a classical controller. To control any system using FLC, the designer needs rules. The rules are defined by an expert with the help of the knowledge they have about the system. And it is a time-consuming task to determine the correct rule and the range of fuzzy variables (Al-Fetyani et al., 2021). The main limitation of FLC is its dependence on an expert's knowledge. ANFIS makes the FLC less dependent on expert and more systematic. The ANFIS generates the linguistic variable ranges of FLC automatically.

4.2.2. ANFIS controller

ANFIS possesses the fundamentals of both the FLC and ANN. Consequently, by merging the benefits of both approaches, it has provided a powerful capability to capture the reasoning capability of FLC and the learning capability of ANN in a single architecture (Subha & Nagalakshmi, 2021). Implementing ANFIS, in essence, provides automatic adjustment of the membership functions of the Sugeno FIS based on training (Oubehar et al., 2018). To get a better understanding of the ANFIS structure, a simplified architecture of ANFIS is shown in figure 4.8, with two inputs (e and de) ,two MFs (A and B), and four rules, as well as four MFs of the output.

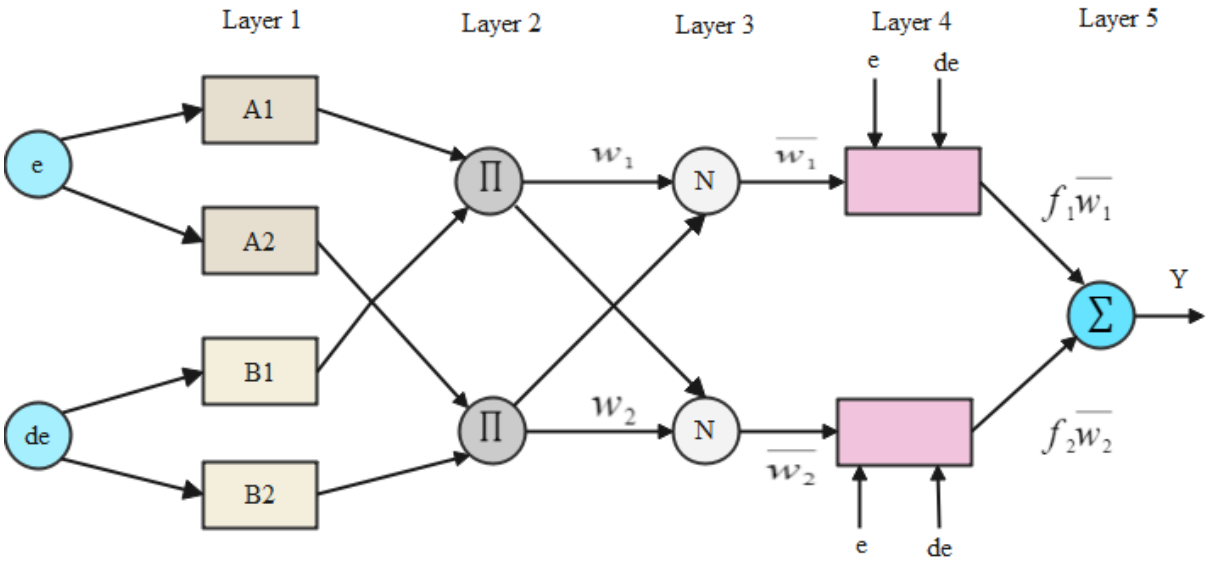

Figure 4. 8 ANFIS structure (Housny et al., 2020)

Layer 1: This layer is also referred to as the antecedent or fuzzification layer. It is the layer by which the membership function is assigned to each node of error and rate of change of error. The two inputs of layer one are represented as:

$$\begin{cases} O_i^1 = \mu_{Ai}(e) \\ O_i^1 = \mu_{Bi}(de) \end{cases} \text{ for i=1,2} \tag{4.14}$$

Where e and de are inputs, A_i and B_i are linguistic variables assigned to each node of error and rate of change of error, and μ is the membership function. The different membership functions used in the fuzzy inference mechanism are explained in the literature (Mathworks, 2020). The type of membership function chosen in this thesis is the gaussian membership function, and it is represented by:

$$\begin{cases} \mu_A(e) = \dfrac{-(e-c)^2}{2\sigma^2} \\ \mu_B(de) = \dfrac{-(de-c)^2}{2\sigma^2} \end{cases} \tag{4.15}$$

Layer 2: This layer is also referred to as the rule layer. It is a layer in which the firing strength (weight) is assigned to each node, and it is represented by the following equation:

$$O_i^2 = wi = \mu_{Ai}(e)\mu_{Ai}(de) \tag{4.16}$$

Layer 3: The third layer is the layer by which the firing strength is normalized, and it is represented by the equation below:

$$O_i^3 = \overline{w}_i = \frac{w_i}{w_1 + w_2} \tag{4.17}$$

Layer 4: This layer is also known as the consequent layer. It is the layer by which the output is generated and it is defined by:

$$O_i^4 = \overline{w}_i f_i = \overline{w}_i (q_i e + q_i de + r_i) \tag{4.18}$$

q_i, q_i, and r_i are the parameters of consequent.

Layer 5: This layer is a fixed output layer. In this layer, an overall output is obtained by summing all the incoming inputs, and it is represented by:

$$O_i^5 = \sum_i \overline{w}_i f_i = \frac{\sum_i w_i f_i}{\sum_i w_i} \tag{4.19}$$

Every node in layer one and four is an adaptive node whose parameters are updated in such a way that the demanded mapping between input and output is achieved (Oubehar et al., 2018). In the ANFIS learning algorithm, the optimal relationship between the two inputs (error and rate of change of error) and the output is obtained by optimally tuning the parameters of the antecedent (layer one) and consequent (layer four). In this thesis, the learning algorithm that has been used is a hybrid, which is a combination of the least squared mean error and a back propagation learning algorithm. The least square is a forward pass which is used to identify the parameters of the consequent, whereas in the back propagation method, the error propagates backward so that the parameters of the premises are updated (Subha & Nagalakshmi, 2021)(Oubehar et al., 2018).

4.3.3.1. ANFIS system design on MATHLAB

The steps that are followed to design the ANFIS system on MATHLAB are presented in Figure 4.9. In order for the FIS to be trained, the desired input-output data of the modeled system is loaded. The loaded data set has to be in the form of an array which is arranged in columns as a column vector, and the data in the last column is output data. Then, based on the loaded data, the FIS file is generated. Then an optimization (learning) algorithm is chosen. Finally, the training is started.

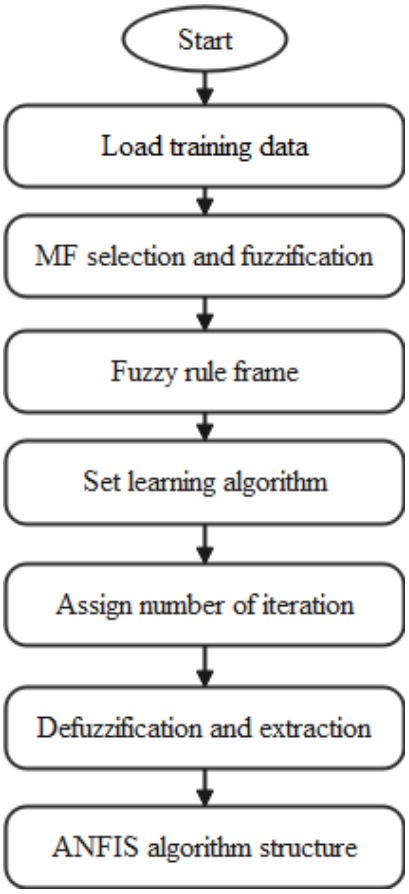

Figure 4. 9 Flow chart of ANFIS algorithm (Oubehar et al., 2018)

4.3.3.2. ANFIS design for STHE temperature control system

In order to design ANFIS for the proposed system, first GA algorithm has been implemented to obtain optimal parameters for PID, which is used to generate the training data. Then, from the GA optimized PID, the error, rate of change of error, and control signal have been taken so that they will serve as input data for the ANFIS training. The training data that has been used for the proposed ANFIS algorithm is represented in figure 4.10.

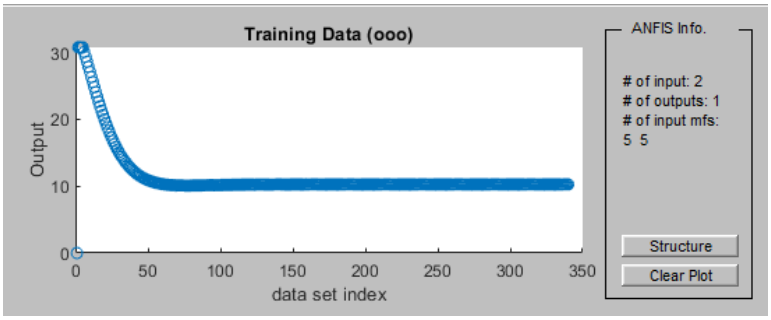

Figure 4. 10 Training data sets for the proposed ANFIS PD algorithm

Table 4. 4 Parameter settings for the developed ANFIS structure

Parameters	Value or type
Number of inputs	2
Number of outputs	1
Number of rules	25
Number of epochs	100
Number of training data pair	340
Number of checking data pair	30
Number of testing data pair	30
Number of output MF	25
Type of output MF	Constant
Type of input MF	Gaussian
Number of input MF	5
Aggregation method	Max
Implication method	Min
And method	Prod
Inference system	Sugeno
Optimization method	Hybrid

Once the training has been completed based on the above specification, the formed rules, the membership function, as well as the output coefficients are generated in sugeno style and saved in the form of *F*IS file. The obtained ANFIS structure and the Mf of the antecedent parameter for the proposed system are represented in figures 4.11 and 4.12, respectively.

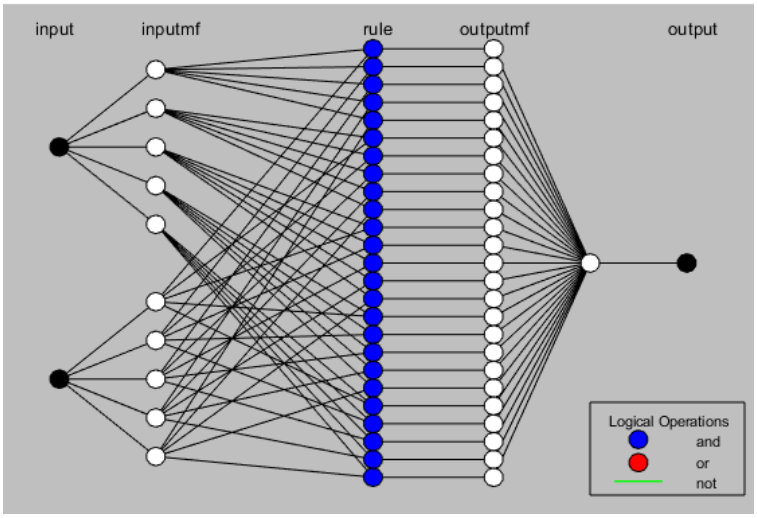

Figure 4. 11 Model structure of the proposed ANFIS controller on MATHLAB

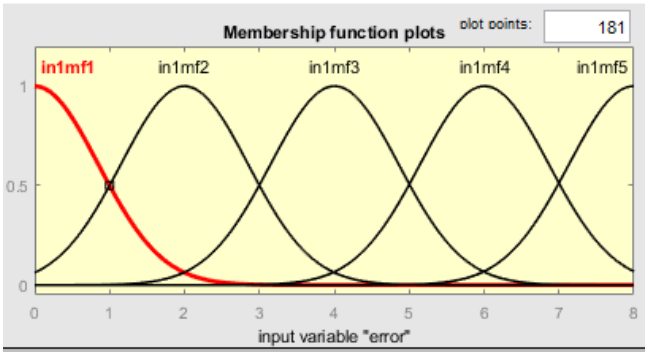

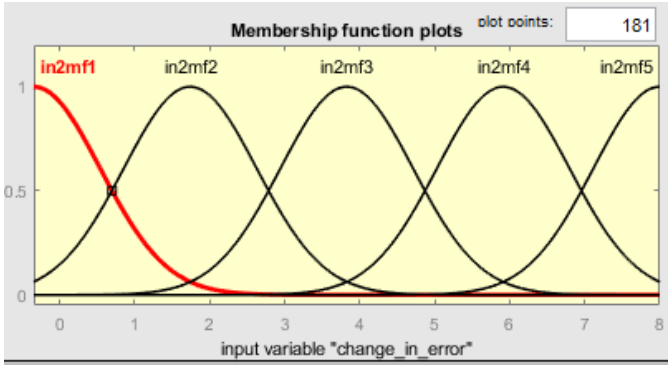

Figure 4. 12 Membership functions of error and rates of change of error

CHAPTER FIVE

RESULT AND DISCUSSION

This chapter consists of six sections. In the first section, a Simulink model of the proposed system is presented. In the second section, the open-loop response of the proposed system is discussed. In the other four sections, the closed-loop response of the proposed system under four scenarios is discussed. The scenarios that are considered are no disturbance, flow variation disturbance, temperature variation disturbance, and both disturbance conditions of the proposed system. Under all the mentioned scenarios, the system is simulated for the set point of $50^{o}c$: This point is chosen because it is within the range of measurement of the sensor.

5.1 Simulink models for the simulation

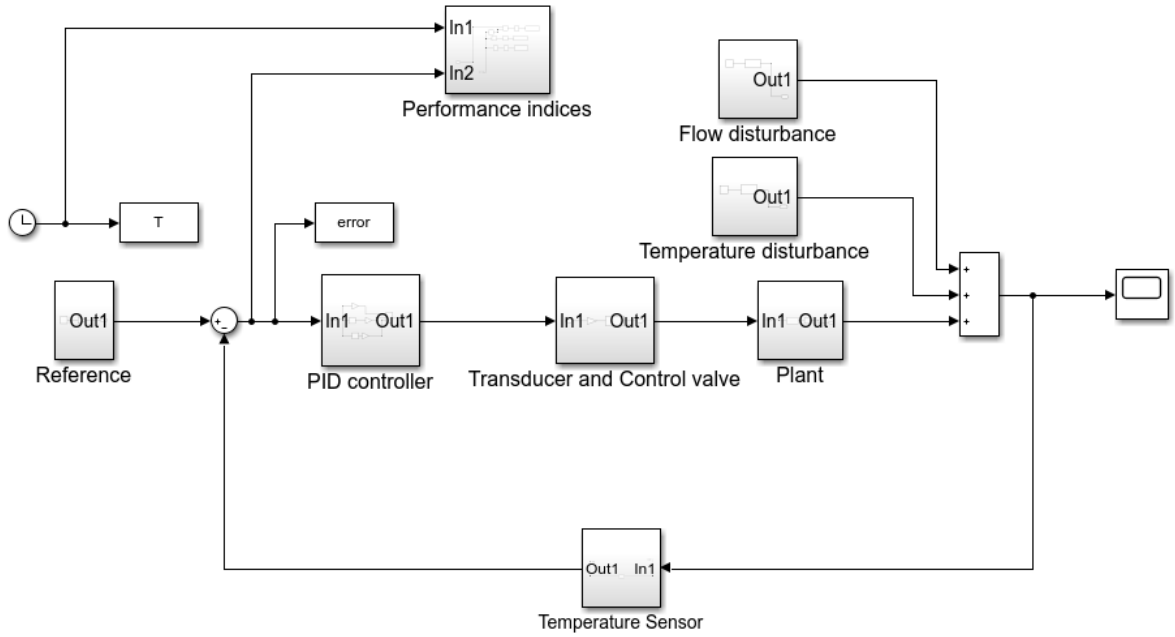

Figure 5. 1 Figure Simulink model of the proposed system using PID controller

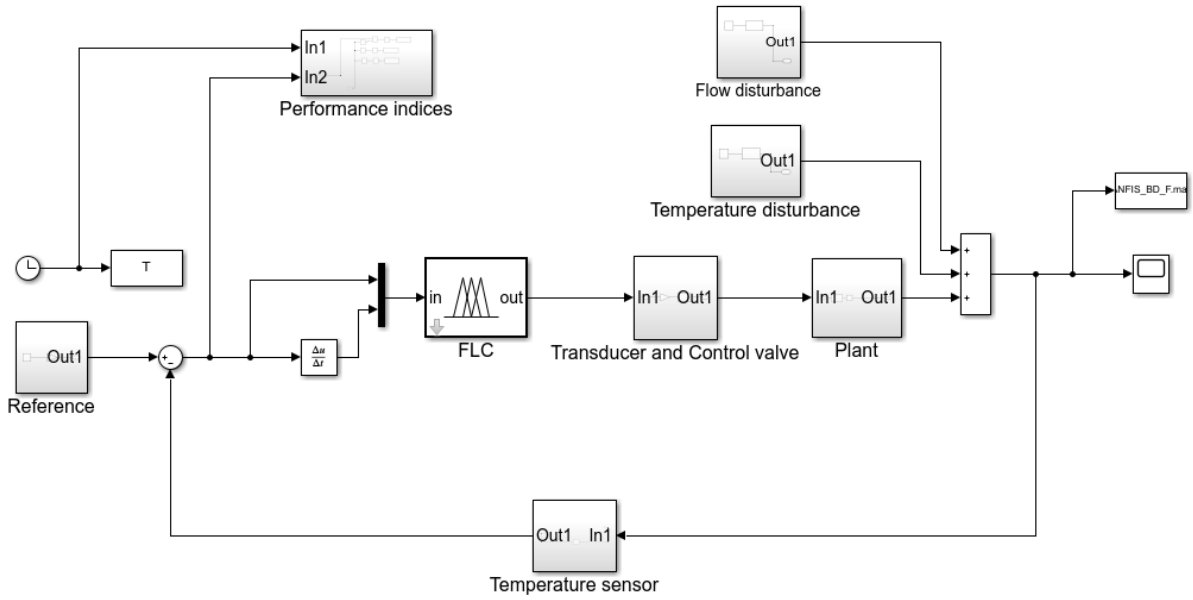

Figure 5. 2 Figure Simulink model of the proposed system using ANFIS PD controller

5.2 Open-loop response of the proposed system

This section clearly illustrates why the closed-loop control system is implemented in all industries to control the temperature of the STHE system. The open-loop response of the proposed system is shown in figure 5.3.

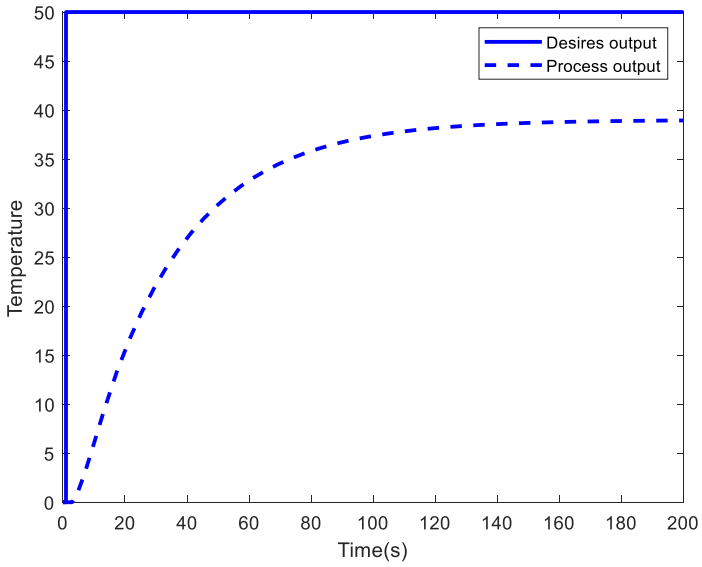

Figure 5. 3 Open-loop response of the proposed system

As can be observed in figure 5.3, the system doesn't settle around the set point, which is the main problem with the heat exchanger temperature control system. The above figure shows that the HE control system is highly subjected to the set point deviation issue and

the amount of steady-state error is very large. Moreover, the system has taken a long time to settle, 120.0541sec. It is obvious that there is a need to implement a closed-loop control strategy. The next sections present the different closed-loop control strategies along with their performance comparison.

5.3. Closed-loop response under no disturbance condition

In this section, the closed-loop response of the proposed system under no disturbance conditions is analyzed using classical ZN_PID, GA_PID, and ANFIS PD controllers. A comparison among the proposed controllers is also done.

5.3.1. Response of ZN tuned PID controller under no disturbance condition

Table 5. 1 Parameter setting of classical PID controller

Parameter	Kp	Ki	Kd
Value	7.1337	0.10563	32.8237

Based on the above parameter setting, the response of the proposed system is obtained as:

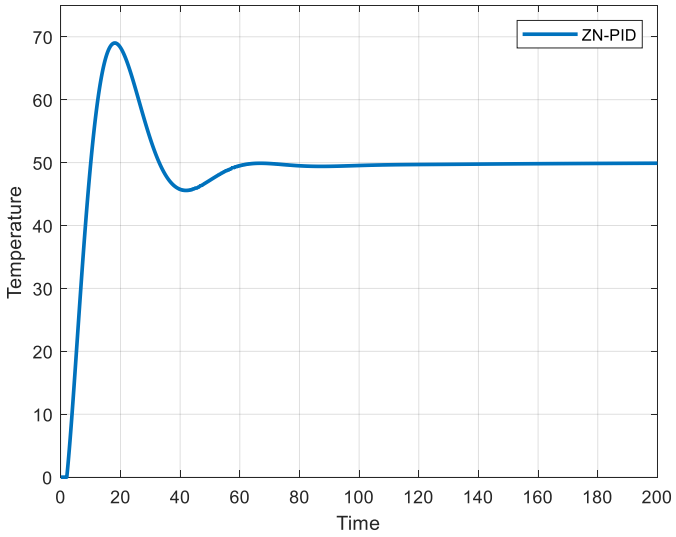

Figure 5. 4 ZN tuned PID response under no disturbance condition

From figure 5.4, we can observe that the proposed system exhibits better performance in terms of steady-state error when a classical PID controller is implemented. However, the system has taken a long time to settle (55.6008sec), which indicates that more time has been taken to track the set point. Additionally, it exhibits the presence of a large amount of

percentage overshoot (38.2921%), which is undesirable. The performance measure of the classical PID controller is summarized in table 5.2.

Table 5. 2 Performance measure of ZN_PID controller under no disturbance condition

Controller	Performance measure		
	Settling Time	Percentage overshoot	IAE
ZN_PID	55.6008sec	38.2921%	117.7

From Table 5.2, it can be concluded that even though the classical PID controller has eliminated steady-state error, it results in a longer settling time and high overshoot. These parameters are critical in process control.

5.3.2. Response of GA tuned PID under no disturbance condition

In table 5.3, GA tuned PID gains based on minimizing IAE, ITAE, and ISE objective functions are represented.

Table 5. 3 GA optimized PID gains for the three objective functions

Gains / J	Kp	Ki	Kd
J1=IAE	5.9982	0.1061	37.0577
J2=ISE	5.9981	0.1239	49.9871
J3=ITAE	4.2458	0.0813	28.1850

Based on the above parameter settings, the simulation result is shown in the figure below.

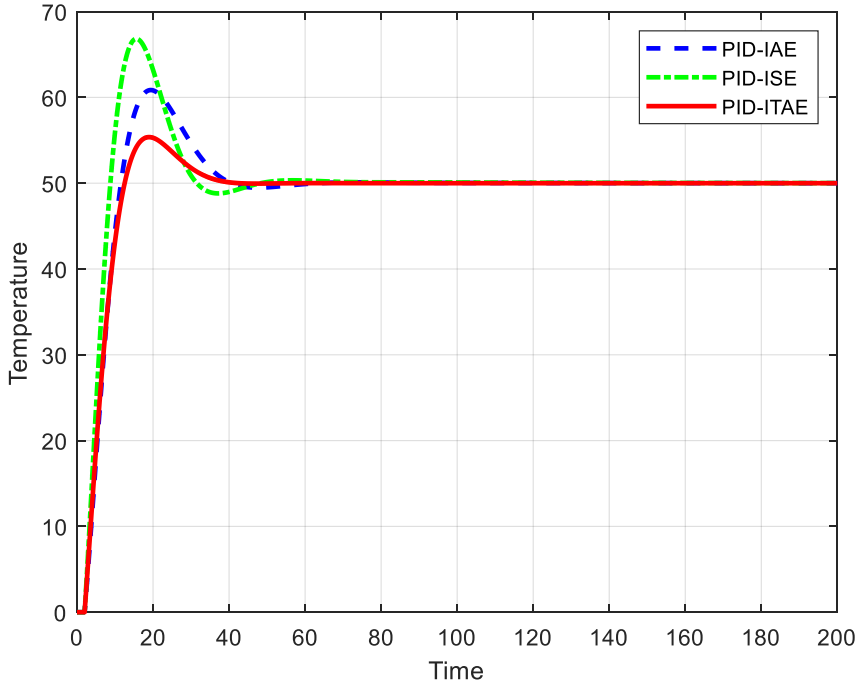

Figure 5. 5 GA tuned PID response under no disturbance condition

From the simulation result shown in figure 5.5, it can be understood that the PID controller tuned using a GA has eliminated the steady-state error. The performance of the PID controller tuned based on minimizing the ITAE objective function results in better performance than the one tuned based on minimizing ISE and the IAE objective function. However, it results in the presence of a certain amount of peak overshoot during the initial response time. The performance measures are summarized in table 5.4.

Table 5. 4 Performance measure of GA_PID controller under no disturbance condition

Controllers	Performance measure		
	Settling time	Percentage overshoot	IAE
PID-ISE	40.3091sec	33.6136%	94.3
PID-IAE	36.8457sec	21.6960%	108.7
PID-ITAE	32.9412sec	10.7433%	111.2

From table 5.4, it can be clearly observed that GA PID tuned based on minimizing ISE objective function exhibits an overshoot of 33.61%. This overshoot has been reduced to 21.69%, an improvement of 35.5% by tuning the gains of PID based on minimizing the IAE objective function. Even though the overshoot has decreased to some extent, it can be

further minimized to 10.7% by tuning the gains of the PID based on minimizing the ITAE objective function. In GA_PID tuned based on minimizing the ISE objective function, the settling time was 40.3091sec, whereas in GA-based PID tuned using the IAE objective function, the settling time has been minimized to 36.8457sec, an improvement of 8.6%. This overshoot is further minimized to 32.94sec using the ITAE objective function.

Table 5.4 also depicts the existence of a trade-off between transient response criteria and error-based criteria in the STHE temperature control system. The ISE objective function has the least IAE value compared to the one tuned using other objective functions, but results in a high amount of overshoot and longer settling time.

5.3.3 Response of ANFIS PD controller under no disturbance condition

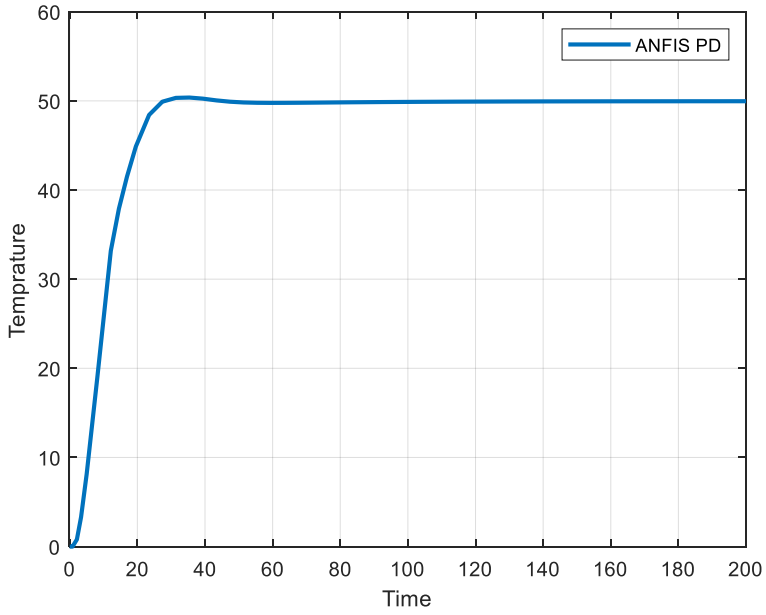

Figure 5. 6 ANFIS PD response under no disturbance condition

From Figure 5.6, it can be clearly observed that the ANFIS PD controller has the best performance in tracking the set point within the shortest period. Additionally, the percentage overshoot is very small. The performance measures of the ANFIS PD controller are summarized in table 5.5.

Table 5. 5 ANFIS PD performance measures under no disturbance condition

Controllers	Performance measure		
	Settling Time	Percentage overshoot	IAE
ANFIS_PD	25.0448sec	0.9007%	139.9

From table 5.5, it can be clearly observed that the ANFIS PD controller provides the best performance despite the nonlinearity of the proposed system. The settling time and percentage overshoot are 25.0448 s and 0.9007%, respectively.

5.3.4. Performance comparison of the proposed controllers under no disturbance condition

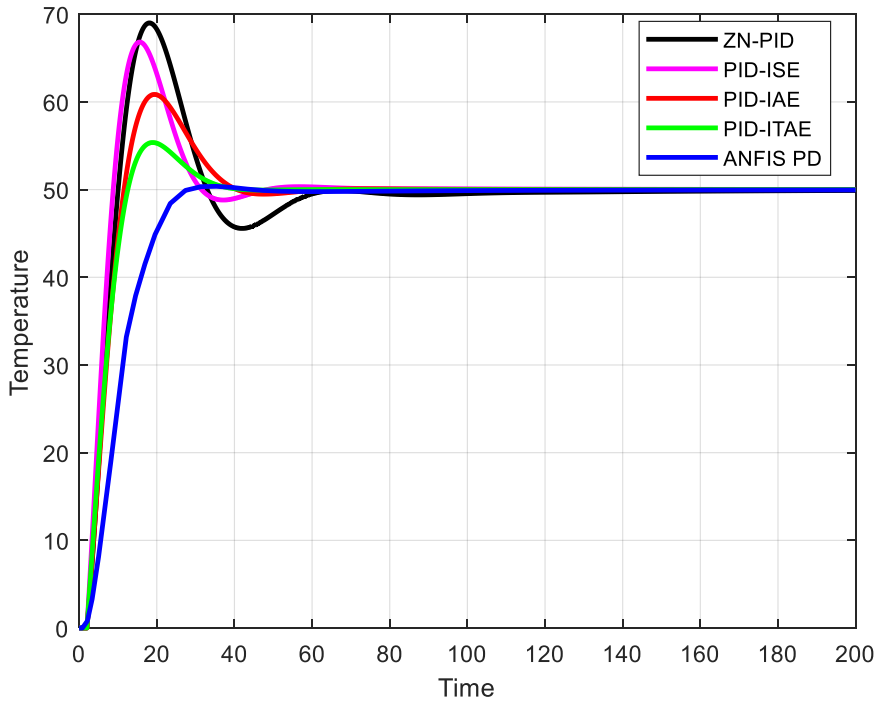

Figure 5.7 performance comparison of the proposed controllers under no disturbance condition

From the above figure 5.7 we it can be clearly observed that the overall performance of ANFIS PD is better when compared to other controllers. The performance comparisons of the proposed controllers are summarized in table 5.6 and bar chart shown in figure 5.8 below.

Table 5. 6 Performance measures of the proposed controllers under no disturbance scenario

Controller	Performance measure		
	Settling time	Maximum overshoot	IAE
ZN-PID	55.6008sec	38.2921%	117.7
PID-ISE	40.3091sec	33.6136%	94.3
PID-IAE	36.8457sec	21.6960%	108.7
PID-ITAE	32.9412sec	10.7433%	111.2
ANFIS PD	25.0448sec	0.9007%	139.9

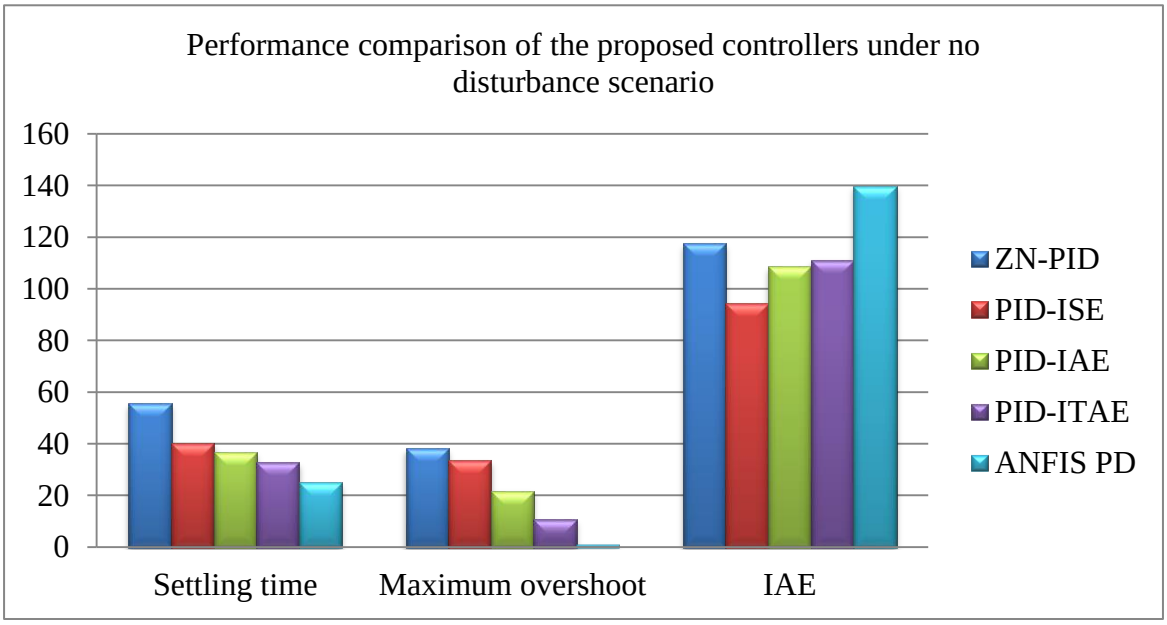

Figure 5. 8 Bar chart representation under no disturbance condition

From the above figure and table, it can be clearly observed that ANFIS PD has got the best performance in terms of transient response criteria. However, it has more IAE value compared to the other controllers. In contrast, GA based PID tuned based on minimizing ISE objective function has the least IAE value compared to the others, but results in poor performance in terms of maximum overshoot and settling time. Therefore, if the target of the control loop is only to reduce IAE and doesn't take into consideration transient response criteria, it is recommended to use GA_PID tuned based on minimizing ISE. But

practically, most control loops focus on improving the maximum overshoot and settling time.

Another conclusion to be drawn from the above table is that even the best controller does not meet all of the criteria at the same time. The performance of ANFIS PD, for example, is far superior to that of other controllers, but it has a higher IAE value than the others

5.4. closed-loop responses subjected to flow variation disturbance

5.4.1. Response of ZN tuned PID controller subjected to flow variation disturbance

In this thesis the considered flow variation disturbance is 13% of the set point.

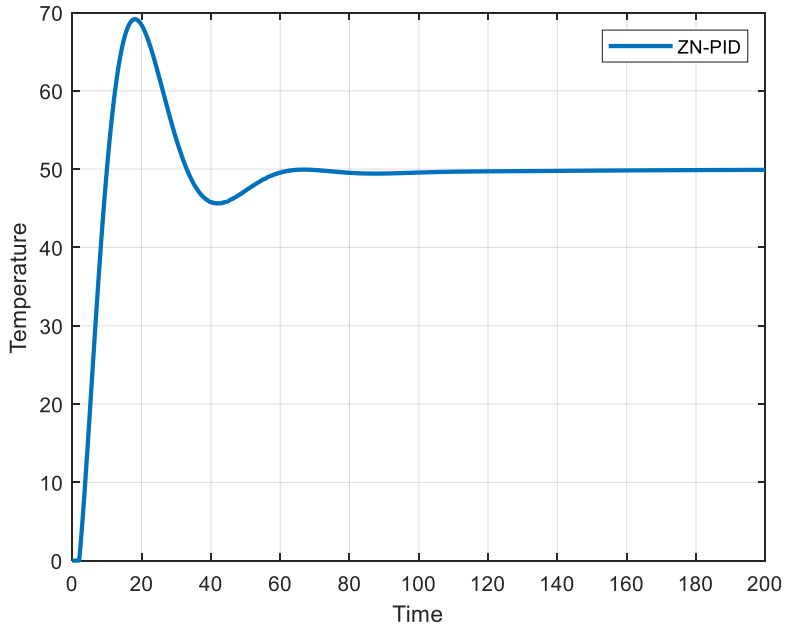

Figure 5. 9 ZN tuned PID response under flow disturbance condition

Table 5. 7 Performance measure of ZN_PID controller under flow disturbance condition

Controller	Performance measure		
	Settling Time	Percentage overshoot	IAE
ZN PID	56.7950ses	38.5499	118.1

5.4.2 Response of GA based PID subjected to flow variation disturbance

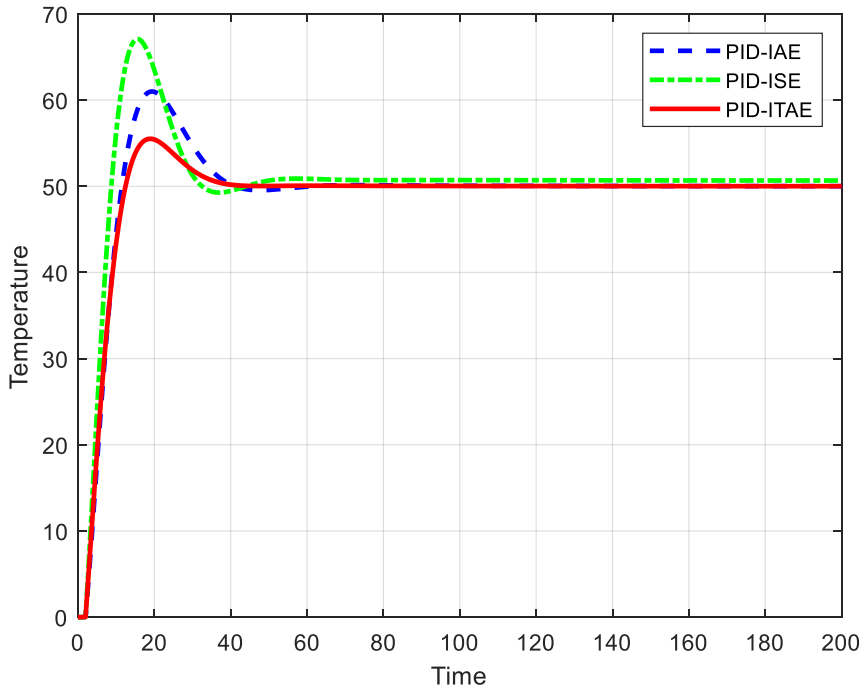

Figure 5. 10 GA tuned PID response under flow disturbance condition

From figure 5.10, it can be clearly observed that even with the existence of a flow disturbance effect, the performance of GA_PID tuned based on minimizing ITAE objective function is superior to the others. Another conclusion drawn from the graph is that when the proposed system is subjected to flow variation disturbance, the ISE objective function produces very little steady state error.

Table 5. 8 Performance measure of GA_PID controller under flow disturbance condition

Controllers	Performance measure		
	Settling time	Percentage overshoot	IAE
PID-ISE	41.5811sec	32.3967%	94.3
PID-IAE	37.0463sec	21.9630%	109.3
PID-ITAE	33.3557sec	11.0030%	111.9

From table 5.8, it can be observed that when the system is subjected to flow disturbance, the least settling time and overshoot are observed when the system is tuned based on

minimizing the ITAE objective function, having numerical values of 33.3557sec and 11.003%, respectively. In contrast, the highest settling time and maximum overshoot are observed under the ISE objective function. The transient state performance of the IAE objective function is between ITAE and ISE. The other conclusion to be drawn from the above table is that the minimal IAE is observed when the ISE objective function is used.

5.4.3. Response of ANFIS PD controller subjected to flow variation disturbance

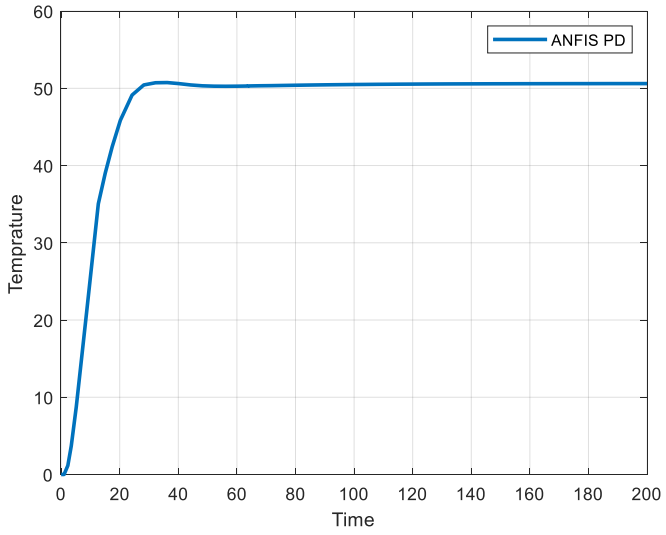

Figure 5. 11 ANFIS PD response under flow disturbance condition

From figure 5.11, it can be clearly observed that the overall performance of the ANFIS PD controller is best even in the presence of a flow variation disturbance effect. The other thing that can be observed from the above figure is that under flow disturbance conditions, the ANFIS PD controller results in a very small amount of steady state error.

Table 5. 9 ANFIS PD performance measures under flow disturbance condition

Controllers	Performance measure		
	Settling Time	Percentage overshoot	IAE
ANFIS_PD	25.4396sec	0.4621%	145.3

From table 5.9, it can be understood that the overall performance of ANFIS PD is good even in the presence of flow variation disturbance. The decrease in percentage overshoot results due to the fact that when the system is subjected to flow disturbance conditions, the ANFIS PD controllers result in a certain amount of steady state error.

5.4.4 Performance comparison of the proposed controller under flow variation disturbance

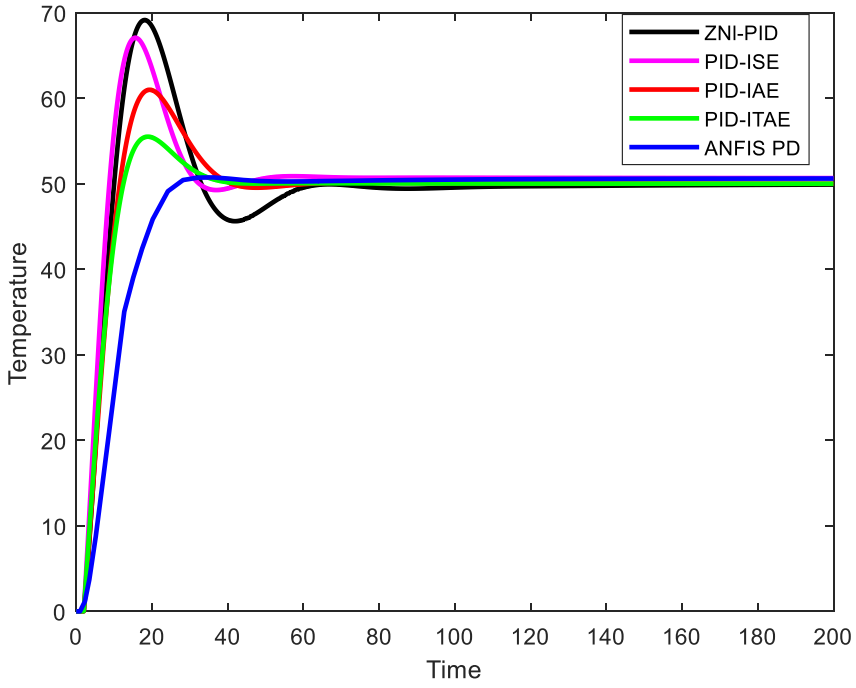

Figure 5. 12 Performance comparison of the proposed controllers under flow disturbance

From figure 5.12, it can be clearly observed that ANFIS PD has got better transient response even in the presence of flow variation disturbance. The performance comparisons of the proposed controllers are summarized in table 5.10 and bar chart shown in figure 5.13.

Table 5. 10 Performance measures of the proposed controllers under flow disturbance

Controllers	Performance measure		
	Settling time	Percentage overshoot	IAE
ZN PID	56.7950ses	38.5499%	118.1
PID-ISE	41.5811sec	32.3967%	94.3
PID-IAE	37.0463sec	21.9630%	109.3
PID-ITAE	33.3557sec	11.0030%	111.9
ANFIS-PD	25.4396sec	0.4621%	145.3

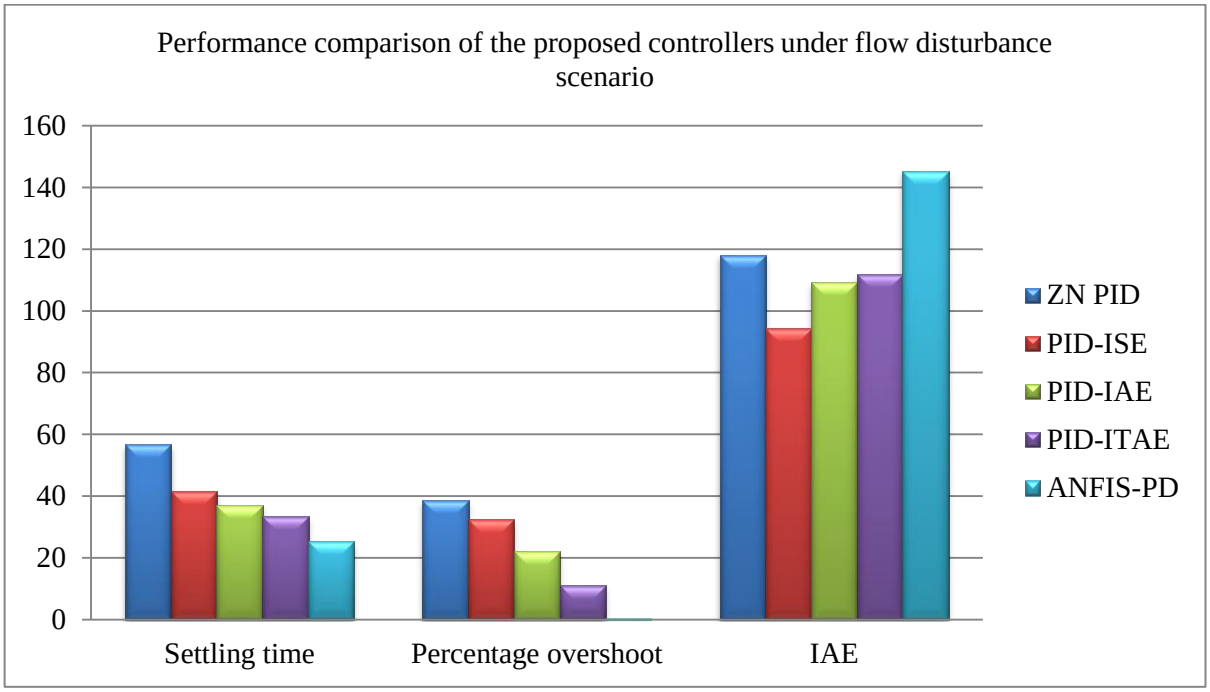

Figure 5. 13 Bar chart representation under flow disturbance scenario

5.5. Closed loop response subjected to temperature variation disturbance

In this thesis the considered temperature variation disturbance is 13% of the set point

5.5.1. Response of ZN_PID controller subjected to temperature variation disturbance

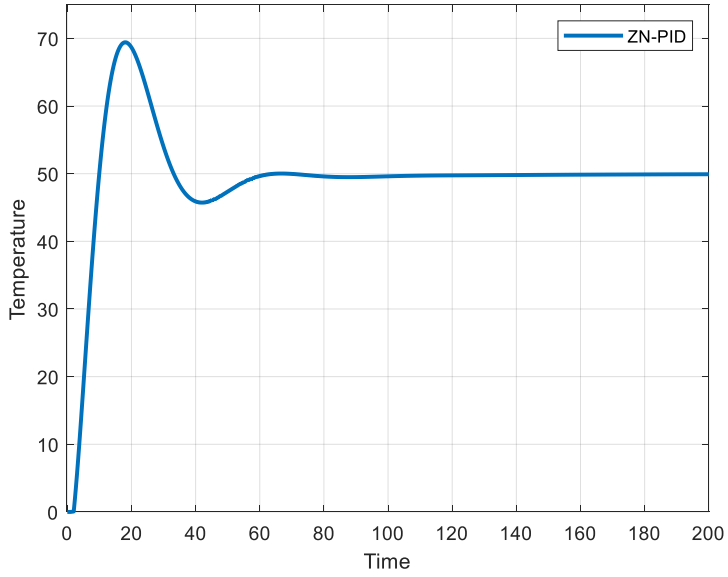

Figure 5. 14 ZN tuned PID response under temperature disturbance condition

Table 5. 11 Performance measure of ZN_PID under temperature disturbance

Controllers	Performance measure		
	Settling time	Percentage overshoot	IAE
ZN_PID	57.1933sec	39.0657%	119.3

From table 5.11, it can be clearly observed that when the system is subjected to a temperature variation disturbance effect, the settling time, overshoot, and IAE value are 57.1933sec, 39.0657%, and 119.3, respectively.

5.5.2. Response of GA tuned PID subjected to temperature variation disturbance

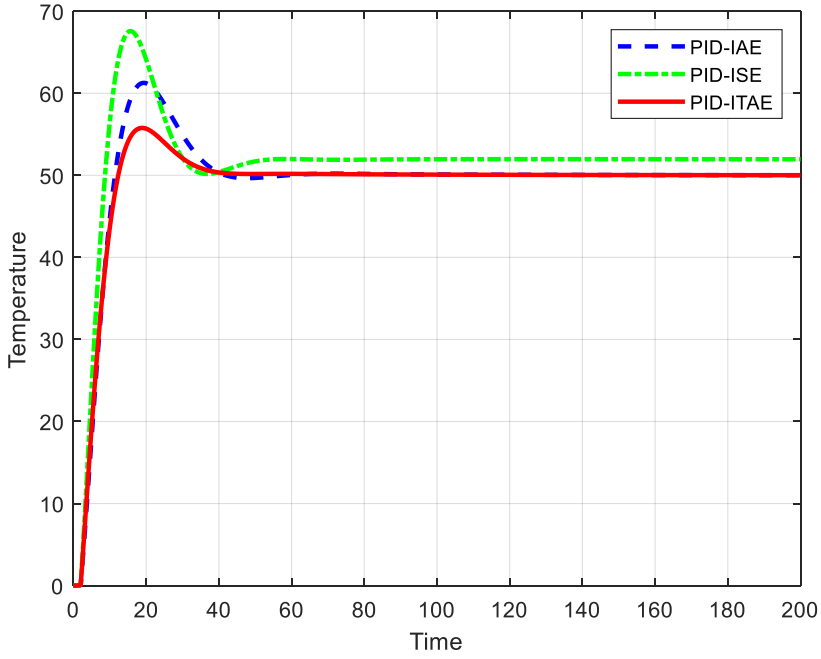

Figure 5. 15 GA tuned PID response under temperature disturbance condition

Figure 5.15 depicts that even with the presence of temperature variation disturbance effect, the performance of GA_PID tuned based on minimizing ITAE objective function is better when compared to the others. When the system is subjected to a temperature variation disturbance effect, the resultant steady state error is greater than the one that has occurred in the flow disturbance condition. The performance measures of the three objective functions are summarized in the table 5.12.

Table 5. 12 Performance measure of GA_PID under temperature disturbance condition

Controllers	Performance measure		
	Settling Time	Percentage overshoot	IAE
PID-ISE	43.6267sec	30.0560%	94.3
PID-IAE	37.4588sec	22.4973%	110.6
PID-ITAE	34.2404sec	11.5226%	112.1

From the above table, it can be observed that when the system is subjected to temperature variation disturbance, the least settling time and overshoot are observed under the ITAE objective function, having numerical values of 34.2404sec and 11.523%, respectively. In contrast, the highest settling time and maximum overshoot are observed under the ISE objective function, with numerical values of 43.6267sec and 30.0560%. The transient state performance of the IAE objective function is between ITAE and ISE. A minimal IAE is observed when ISE is used as an objective function.

5.5.3. Response of ANFIS PD subjected to temperature variation disturbance

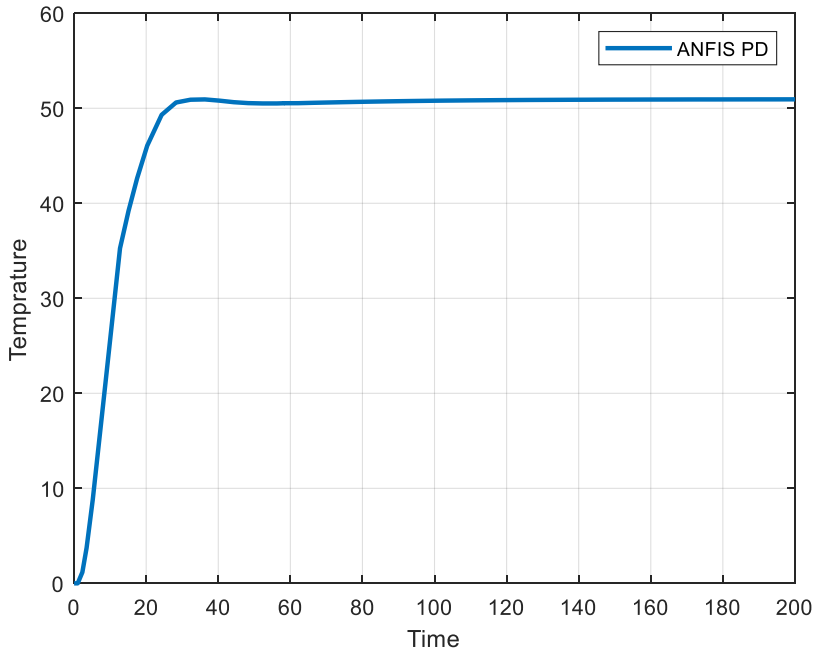

Figure 5. 16 ANFIS PD response under temperature disturbance condition

Table 5. 13 ANFIS PD performance measures under temperature disturbance condition

Controllers	Performance measure		
	Settling time	Percentage overshoot	IAE
ANFIS_PD	26.9480sec	0.1226%	150.8

From the above figure and table, it can be understood that the overall performance of ANFIS PD is good even in the presence of temperature variation disturbance. The overshoot has been eliminated because the temperature variation disturbance has resulted in a certain amount of steady state error.

5.5.4. Performance comparison of the proposed controller under temperature variation disturbance

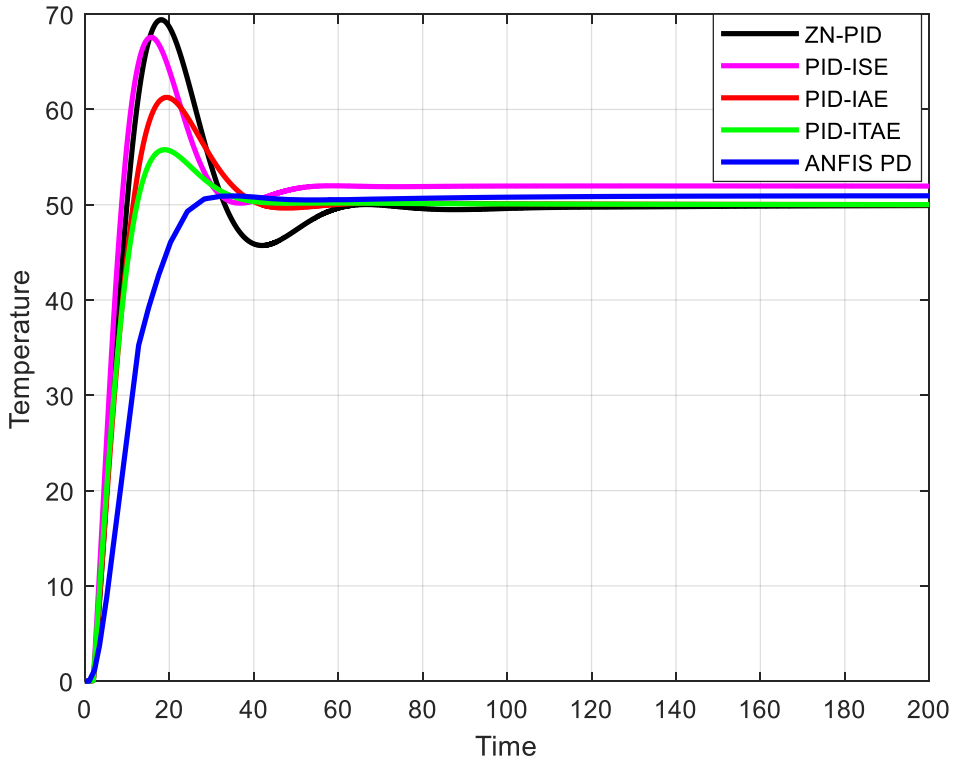

Figure 5. 17 Performance comparison of the proposed controllers under temperature disturbance condition

From figure 5.17, it can be clearly observed that ANFIS PD has got better performance in terms of transient response criteria even in the presence of temperature variation disturbance. However, it has more IAE value compared to the other controllers. In contrast, the GA_PID based on minimizing the ISE objective function has the lowest IAE value

compared to the others, but results in poor performance in terms of maximum overshoot and settling time. The performance comparisons of the proposed controllers are summarized in table 5.14 and bar chart shown in figure 5.18.

Table 5. 14 Performance measures of the proposed controllers under temperature disturbance

Controllers	Performance measure		
	Settling Time	Percentage overshoot	IAE
ZN_PID	57.1933sec	39.0657%	119.3
PID-ISE	43.6267sec	30.0560%	94.3
PID-IAE	37.4588sec	22.4973%	110.6
PID-ITAE	34.2404sec	11.5226%	112.1
ANFIS PD	26.9480sec	0.12265%	150.8

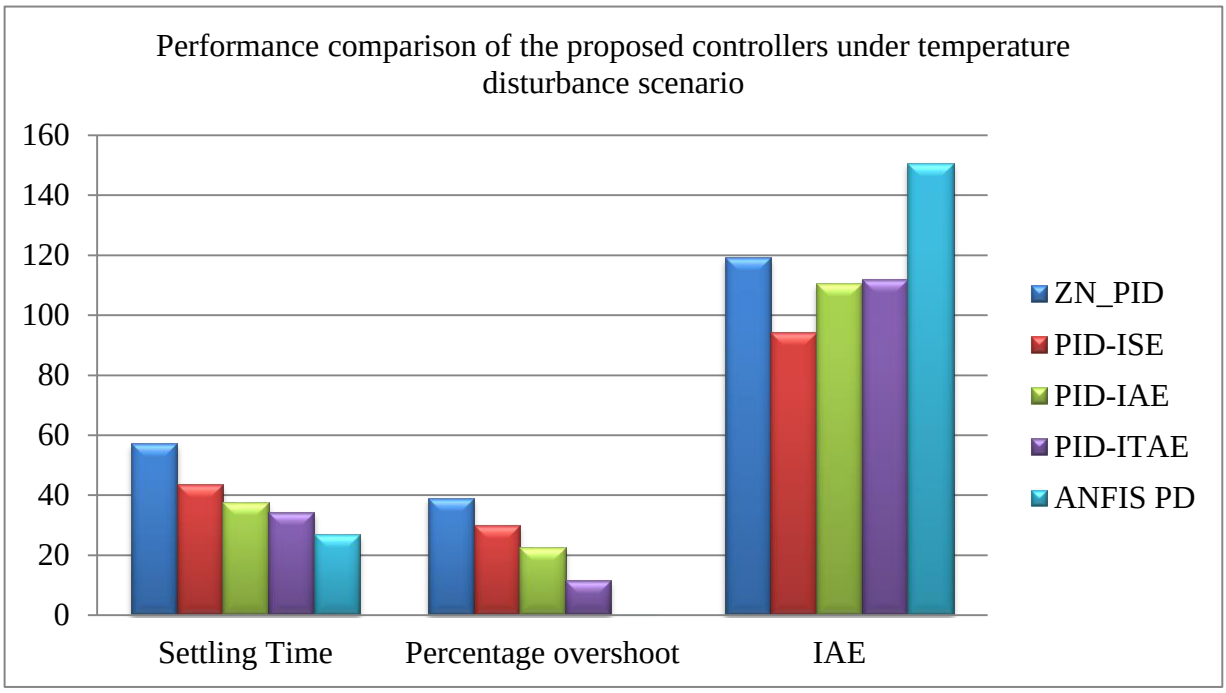

Figure 5. 18 Bar chart representation under temperature disturbance scenario

5.6. Responses of the proposed controllers subjected to both disturbances

5.6.1. Response of ZN tuned PID controller subjected to both disturbances

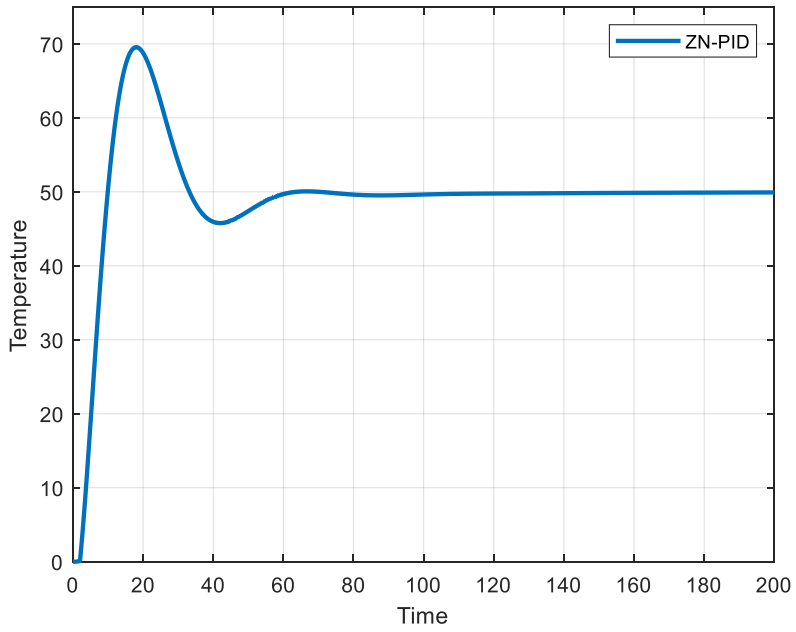

Figure 5. 19 ZN tuned PID response under both disturbance conditions

Table 5. 15 Performance measure of ZN_PID under both disturbance conditions

Controllers	Performance measure		
	Settling time	Percentage overshoot	IAE
ZN PID	58.3978sec	39.3236%	119.9

From table 5.15, it can be clearly observed that when the system is subjected to both temperature and flow variation disturbance, the proposed system's settling time, overshoot, and IAE value are 58.3978sec, 39.3245%, and 119.9, respectively.

5.6.2. Response of GA tuned PID controller subjected to both disturbances

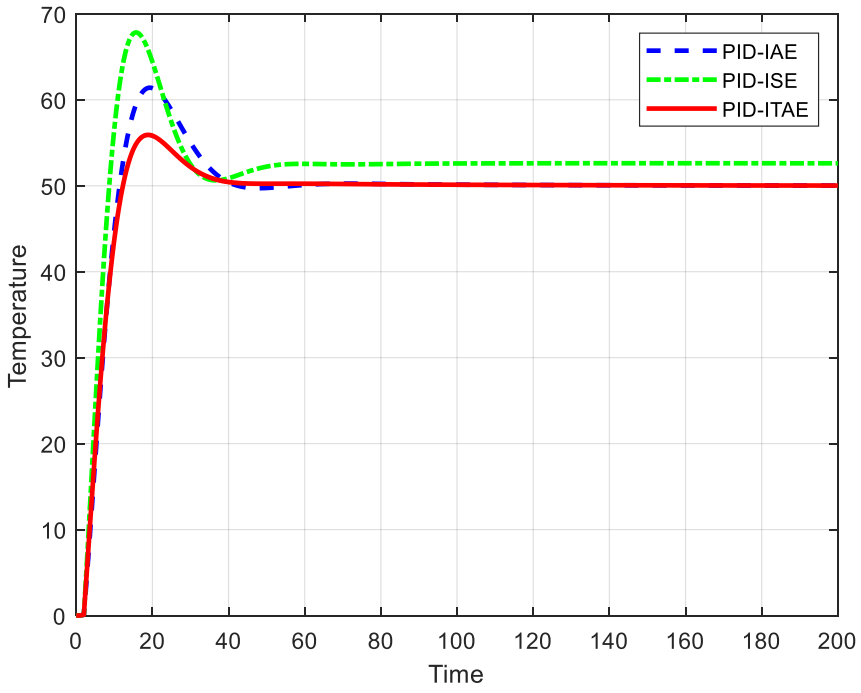

Figure 5. 20 GA tuned PID response under both disturbance condition

Figure 5.20 shows that, even when both temperature and flow variation disturbance effects are present, the performance of the GA_PID controller tuned based on minimizing the ITAE objective function outperforms the one tuned based on minimizing the ISE and the IAE objective functions.

Table 5. 16 Performance measure of GA_PID controller under both disturbance condition

Controllers	Performance measure		
	Settling Time	Percentage overshoot	IAE
PID-ISE	44.5518sec	28.9300%	94.3
PID-IAE	37.6711sec	22.7646%	111.2
PID-ITAE	34.7165sec	11.7824%	112.7

From table 5.16, it can be clearly observed that GA PID tuned based on minimizing ISE objective function exhibits an overshoot of 28.93%. This overshoot has been reduced to 22.7646% by tuning the gains of PID based on minimizing the IAE objective function. Even though the overshoot has decreased to some extent, it can be further minimized to 11.7824% by tuning the gains of the PID based on minimizing the ITAE objective

function. In GA_PID tuned based on minimizing the ISE objective function, the settling time was 44.5518sec, whereas in GA_PID tuned using the IAE objective function, the settling time has been minimized to 37.671sec. The settling time is further minimized to 34.7165sec using the ITAE objective function.

5.6.3. Response of ANFIS PD controller subjected to both disturbances

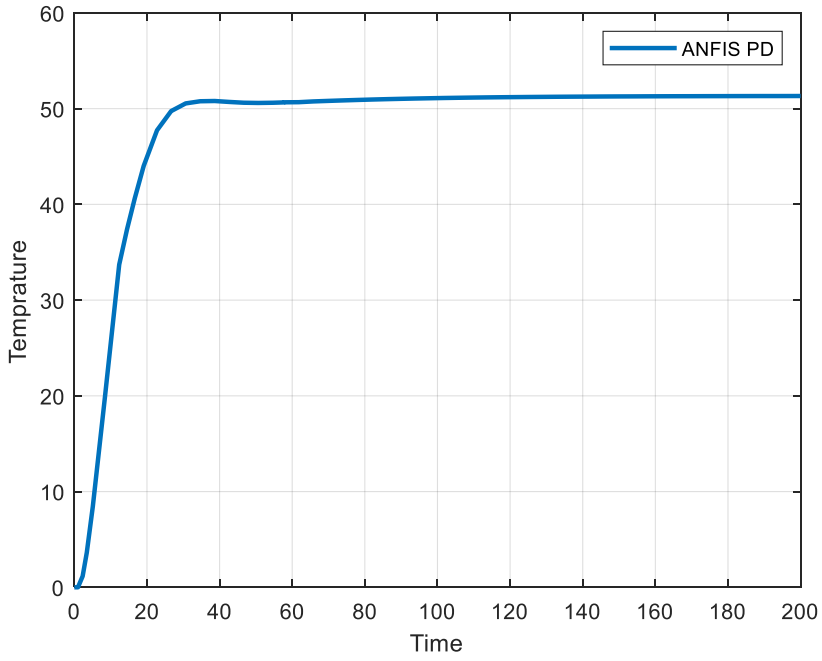

Figure 5. 21 ANFIS PD response under both disturbance condition

From Figure 5.21, it can be clearly observed that the performance of the ANFIS PD controller is still good with the presence of both temperature and flow variation disturbances. As shown in the figure above, when the system is subjected to both disturbance conditions, it results in some steady-state error, but the error is within the acceptable range of operation. The performance measures of ANFIS PD are summarized in table 5.17.

Table 5. 17 ANFIS PD performance measures under both disturbance condition

Controllers	Performance measure		
	Settling time	Percentage overshoot	IAE
ANFIS PD	27.9320sec	0.00012%	159.6

5.6.4. Performance comparison of the proposed controllers under both disturbance conditions

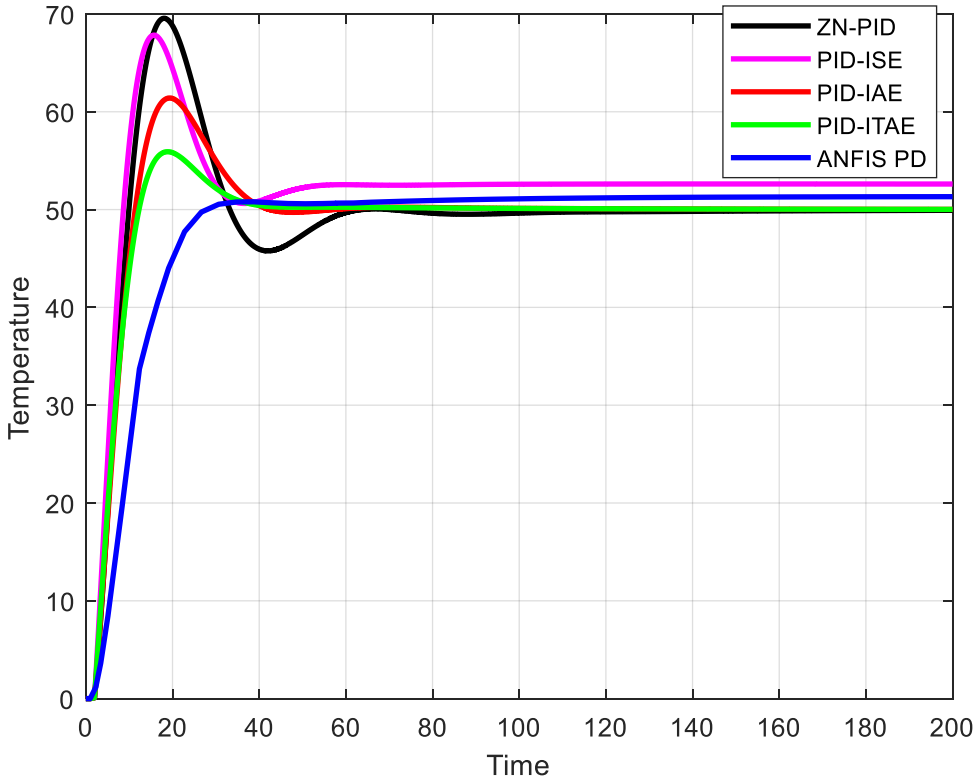

Figure 5. 22 Performance comparison of the proposed controllers under both disturbance condition

Table 5. 18 Performance measures of the proposed controllers under both disturbance

Controllers	Performance measure		
	Settling Time	Percentage overshoot	IAE
ZN-PID	58.3978sec	39.3236%	119.9
PID-ISE	44.5518sec	28.9300%	94.3
PID-IAE	37.6711sec	22.7646%	111.2
PID-ITAE	34.7165sec	11.7824%	112.7
ANFIS PD	27.9320sec	0.00012%	159.6

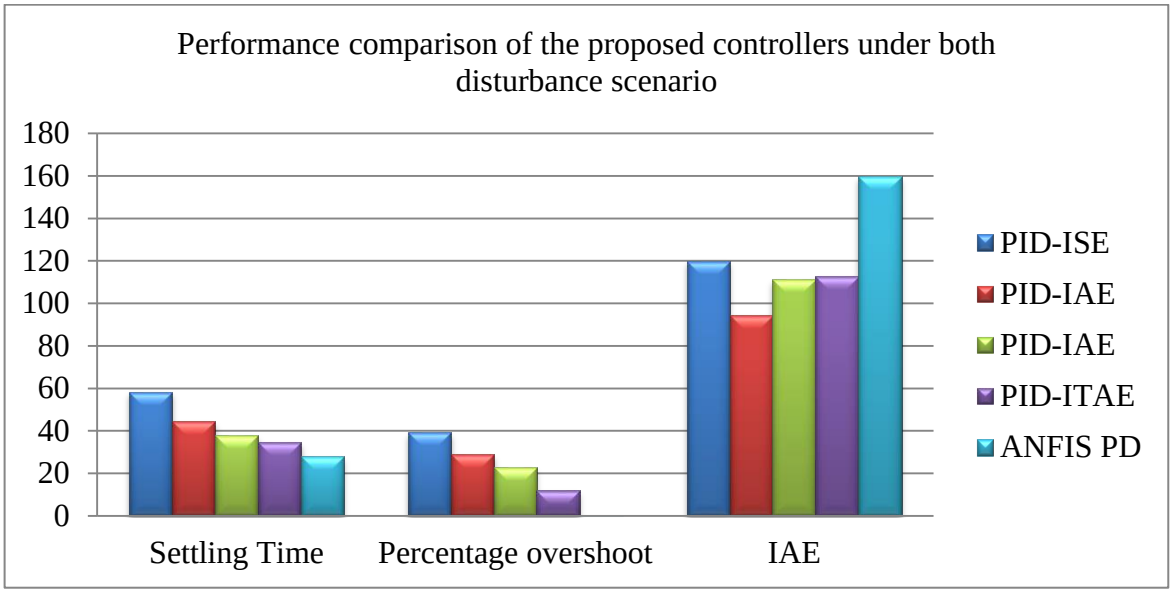

Figure 5. 23 Bar chart representation under both disturbance scenario

From table 5.18, it can be clearly observed that the best transient performance has been found when ANFIS PD is implemented. The settling time and percentage overshoot of the ANFIS PD controller have been found to be 27.9sec and 0.00012% respectively. Whereas the least transient performance has been found when a ZN PID controller is implemented. The least IAE value has been found when GA PID based on minimizing ISE objective function is implemented.

Simulation result summary

From the obtained result and the analysis made the following points have been concluded

- ✓ The overall performance of the ANFIS PD controller is much better with and without the presence of disturbance effect when compared to ZN tuned PID and GA tuned PID controllers within an acceptable range of the IAE value.
- ✓ The presence of a trade-off between transient response criteria and error-based criteria in STHE temperature control system.
- ✓ Among the three objective functions used in the GA based PID controller, the overall performance of the GA_PID tuned based on minimizing ITAE objective function has been found to be the best with and without the presence of disturbance effect**.**

- ✓ Temperature variation disturbance has a more significant effect than flow variation disturbance on a STHE temperature control system.
- ✓ The percentage overshoot of the ANFIS PD and GA_PID tuned based on minimizing ISE objective functions was supposed to increase when the system is subjected to the disturbance effect but has decreased. This is due to the fact that the disturbance causes a certain amount of steady state error. The occurred steady state error has increased the final value and made the overshoot decrease.
- ✓ From the observed simulation result under all the scenarios, namely no disturbance, flow disturbance, temperature disturbance, and both disturbance scenarios, the least IAE value is found when GA_PID based on minimizing ISE objective function is implemented. This is due to the fact that the main goal of this objective function is to penalize large errors.
- ✓ The other thing that can be concluded from the analysis is that even the best controller does not achieve all the mentioned criteria at the same time in STHE temperature control system. For instance, the performance of ANFIS PD is much better than other controllers, but it has more IAE value compared to the other controllers. Therefore, control engineers need to trade-off transient response criteria with error-based criteria of the controlled system so that their requirements are met in a better manner.

6. CONCLUSION AND RECOMMENDATION

6.1 Conclusion

This thesis work has taken a STHE system to compare the performance of different controllers. The controllers that have been taken for comparison purposes are the ZN tuned PID, the GA tuned PID, and the ANFIS PD controller. STHE is chosen because it is an indispensible plant in nuclear power plants, petrochemical, sewage treatment, food processing, beverage, chemical, pharmaceutical, and natural gas processing industries. And the system is highly nonlinear, uncertain, time-delayed, and complex. Moreover, it is accompanied by flow and temperature variation disturbance, which makes it a suitable plant to make an analysis of the proposed controllers.

The PID controller has been tuned using classical ZN tuning method and GA optimization techniques. Three objective functions have been used under genetic algorithms, namely IAE, ITAE, and ISE. Among the three objective functions, ITAE has provided the best performance with and without the presence of the disturbance effect in terms of transient response criteria, whereas the ISE objective function has provided the best performance in terms of error-based criteria when compared to the other two objective functions. The overall performance of GA_PID tuned based on minimizing ITAE objective function is good; however, it results in the presence of overshoot. The settling time and maximum overshoot of the GA_PID tuned based on minimizing ITAE objective function is further minimized using the ANFIS PD controller.

The ANFIS PD is designed in such a way that first the GA optimized PID controller is used so as to obtain the training data set for the ANFIS design. The data sets that are taken for ANFIS training are error, rate of change of error, and control signal. Once the ANFIS structure is obtained, it is implemented into the proposed system.

The performance of the proposed controllers has been compared under four scenarios, namely no disturbance, flow variation disturbance, temperature variation disturbance, and both disturbance conditions. Among the proposed controllers, ANFIS PD has provided the best transient response performance with and without the presence of disturbance effects. Whereas the best error-based performance is obtained when the GA_PID is tuned based on minimizing the ISE objective function. However, it results in a longer settling time and a higher amount of overshoot.

6.2 Recommendation

The parameters of the system specification have been taken from closely related work to compare the performance of the proposed controllers. Testing the controller's performance using real-time data taken from the industry is recommended. Also, the same work can be extended to other non-linear plants in process industries such as distillation columns, continuous stirred tank reactors, boilers, and electric furnaces.

The optimization method that has been used in this thesis is GA optimization techniques, and the work can be extended by implementing other optimization techniques such as Particle Swarm Optimization, the Grey Wolf optimization method, the Local Search Optimization Ant-Colony Optimization (ACO).

Research fund acknowledgment

This research thesis was funded by Adama Science and Technology University under the grant number of ASTU/SM-R/567/22, Adama, Ethiopia.

REFERENCES

Abdullah, Z. (2019). Design and Implementation of Fractional Order Controller for Heat Exchanger. *2019 IEEE 9th International Conference on System Engineering and Technology (ICSET)*, *6*, 453–458.

Ahmmed, T., Akhter, I., Karim, S. M. R., & Ahamed, F. A. S. (2020). *Genetic Algorithm Based PID Parameter Optimization*. *December*.

Al-Fetyani, M., Hayajneh, M., & Alsharkawi, A. (2021). Design of an Executable ANFIS-based Control System to Improve the Attitude and Altitude Performances of a Quadcopter Drone. *International Journal of Automation and Computing*, *18*(1), 124–140. https://doi.org/10.1007/s11633-020-1251-2

Bastida, H., Ugalde-Loo, C. E., Abeysekera, M., Xu, X., & Qadrdan, M. (2019). Dynamic Modelling and Control of Counter-Flow Heat Exchangers for Heating and Cooling Systems. *2019 54th International Universities Power Engineering Conference, UPEC 2019 - Proceedings*, 1–6. https://doi.org/10.1109/UPEC.2019.8893634

Chen, Y. H., & Chang, C. Der. (2018). An intelligent ANFIS controller design for a mobile robot. *Proceedings of 4th IEEE International Conference on Applied System Innovation 2018, ICASI 2018*, *1*, 445–448. https://doi.org/10.1109/ICASI.2018.8394280

Coughanowr, Donald R, S. E. L. (2009). Process systems analysis and control third edition. *McGraw-Hill*, 5. http://www.slideshare.net/accelerate786/process-systems-analysis-and-control-third-edition

Dizaji, N. K., Sakhvati, A., & Hosseini, S. H. (2015). *Design of a PID feed-forward controller for controlling Output fluid temperature in shell and tube hear exchanger*. *3*, 30–34. https://doi.org/10.11648/j.jeee.s.2015030201.17

Dodd, R. (1983). *Thermal design of shell and tube heat exchangers.*

Dutta, D., & Upreti, S. R. (2021). Artificial intelligence-based process control in chemical, biochemical, and biomedical engineering. *Canadian Journal of Chemical Engineering*, *May*, 1–38. https://doi.org/10.1002/cjce.24246

Eldin, A., & Awouda, A. (2017). *Design of Self Tuning PID Controller Using Fuzzy Logic for DC Motor Speed*. *2*(4), 27–33.

Farah, N., H. N. Talib, M., Ibrahim, Z., M. Lazi, J., & Azri, M. (2018). Self-tuning Fuzzy Logic Controller Based on Takagi-Sugeno Applied to Induction Motor Drives. *International Journal of Power Electronics and Drive Systems (IJPEDS)*, *9*(4), 1967. https://doi.org/10.11591/ijpeds.v9.i4.pp1967-1975

G. M. Sarabeevi and M. L. Beebi. (2016). *Temperature control of shell and tube heat exchanger system using internal model controllers*. https://doi.org/10.1109/ICNGIS.2016.7854015

Gani, M., Islam, S., & Ahsan, M. (2019). Optimal PID tuning for controlling the temperature of electric furnace by genetic algorithm. *SN Applied Sciences*, *1*(8), 1–8. https://doi.org/10.1007/s42452-019-0929-y

García-Martínez, J. R., Cruz-Miguel, E. E., Carrillo-Serrano, R. V., Mendoza-Mondragón, F., Toledano-Ayala, M., & Rodríguez-Reséndiz, J. (2020). A PID-type fuzzy logic controller-based approach for motion control applications. *Sensors (Switzerland)*, *20*(18), 1–19. https://doi.org/10.3390/s20185323

Goodwin, G. C., Graebe, S. F., & Salgado, M. E. (2000). *Control System Design*.

Hanke, K. (2007). *Control System Principle and Design* (3rd ed., Issue 1949).

Housny, H., Chater, E. A., & Fadil, H. El. (2020). PSO-based ANFIS for quadrotor system trajectory-tracking control. *2020 1st International Conference on Innovative Research in Applied Science, Engineering and Technology, IRASET 2020*, *1*, 0–5. https://doi.org/10.1109/IRASET48871.2020.9092015

Jamal, A., & Syahputra, R. (2016). Heat exchanger control based on artificial intelligence approach. *International Journal of Applied Engineering Research*, *11*(16), 9063–9069.

Khames, A., Lesewed, A. A., & Al-mathnani, A. O. (2020). *Synthesis of Sliding Mode Control for Heat Exchanger*. *November*, 28–30.

Khan, S. (2017). *Modeling and Controlling Heat Exchanger Process*. Lambert Academic publishing.

Lavine, T. L. B. and A. S. (2017). *Fundamentals of heat and mass transfer* (Eighth edi).

Liu, F., Wang, H., Shi, Q., Wang, H., Zhang, M., & Zhao, H. (2017). Comparison of an

ANFIS and Fuzzy PID Control Model for Performance in a Two-Axis Inertial Stabilized Platform. *IEEE Access*, *5*(8), 12951–12962. https://doi.org/10.1109/ACCESS.2017.2723541

Manipatruni, J. (2018). *Design and Implementation of PID Controller using Genetic Algorithm*. *7*(11), 104–107.

Mathworks, C. (2020). Adaptive Fuzzy Inference System Toolbox. *Mathworks*. https://www.mathworks.com/help/fuzzy/anfis

Meena, D. C. (2017). Genetic Algorithm Tuned PID Controller for Process Control. *IEEE*, 1–6.

Morphet, J. (2017). *Fundamentals of industrial instrumentation and process control*.

Olana, F. D. (2021). *PID Temperature Controller Design for Shell and Tube Heat Exchanger*. *February*, 37–46. https://doi.org/10.5815/ijem.2021.01.05

Oubehar, H., Selmani, A., Archidi, M. H., Lachhab, A., & Bouchikhi, B. (2018). Design and real time implementation of ANFIS controller for greenhouse climate. *2018 International Conference on Electronics, Control, Optimization and Computer Science (ICECOCS)*, 1–4.

Padhee, S. (2014). Controller design for temperature control of heat exchanger system: Simulation studies. *WSEAS Transactions on Systems and Control*, *9*(1), 485–491.

Padhee, S., Khare, Y. B., & Singh, Y. (2011). *Internal Model Based PID Control of Shell and Tube Heat Exchanger System*. 297–302.

Reddy, C. S., & Balaji, K. (2021). *A fuzzy-PID controller in shell and tube heat exchanger simulation modeled for temperature control*. *21*(3), 1364–1371. https://doi.org/10.11591/ijeecs.v21.i3.pp1364-1371

Sarabeevi, G. M., and M. L. B. (2016). Temperature control of shell and tube heat exchanger system using internal model controllers. *IEEE*, *1*(69), 5–24.

Seborg. (2017). Process Dynamics and Control fourth edition. In *Journal of Chemical Information and Modeling* (Vol. 53, Issue 9).

Sharma, C., Gupta, S., & Kumar, V. (2011). Modeling and simulation of heat exchanger used in soda recovery. *Proceedings of the World Congress on Engineering 2011*,

WCE 2011, *2*, 1406–1409.

Somasundar Reddy, C., & Balaji, K. (2020). A Genetic Algorithm (GA)-PID Controller for Temperature Control in Shell and Tube Heat Exchanger. *IOP Conference Series: Materials Science and Engineering*, *925*(1). https://doi.org/10.1088/1757-899X/925/1/012020

Srivastava, N., Alejandro, F., & Torres, M. (2016). *Matlab Simulation of Temperature Control of Heat Exchanger using Different Controllers Related papers*. https://doi.org/10.11648/j.acis.20140201.11

Subha, S., & Nagalakshmi, S. (2021). Design of ANFIS controller for intelligent energy management in smart grid applications. *Journal of Ambient Intelligence and Humanized Computing*, *12*(6), 6117–6127. https://doi.org/10.1007/s12652-020-02180-y

Suthar, H. A. (2017). *Two degree of freedom controller optimization using GAfor shell and tube heat exchanger*. 1–7.

ThayaaSree, P., Mythily, M., Vasanthi, D., & Manamalli, D. (2021). Design and Implementation of Fractional Order PI Controller for FCCU. *Lecture Notes in Electrical Engineering*, *70*(3), 2567–2577. https://doi.org/10.1007/978-981-15-8221-9_239

Tidke, A. (2018). Disturbance Rejection PID controller optimized using Genetic Algorithm for Time Delay systems. *2018 International Conference on Control, Power, Communication and Computing Technologies (ICCPCCT)*, *1*, 245–249.

Tridianto, E., Ariwibowo, T. H., Almasa, S. K., & Prasetya, H. E. G. (2017). Cascaded PID temperature controller for FOPDT model of shell-and-tube heat exchanger based on Matlab/Simulink. *Proceedings IES-ETA 2017 - International Electronics Symposium on Engineering Technology and Applications*, *2017-Decem*, 185–191. https://doi.org/10.1109/ELECSYM.2017.8240400

Tuntas, R. (2019). *A neural network based controller design for temperature control in heat exchanger*. *26*(July), 342–346.

Valarmathi, R. (2018). Design of Genetic Algorithm based Internal Model Controller for a Heat Exchanger. *2018 Internat2018 International Conference on Computation of*

Power, Energy, Information and Communication (ICCPEIC)Ional Conference on Computation of Power, Energy, Information and Communication (ICCPEIC), 489–495. https://doi.org/10.1109/ICCPEIC.2018.8525208

Vasickaninová, A., & Bakošová, M. (2015). Robust controller design for a heat exchanger. *Proceedings of the 2015 20th International Conference on Process Control, PC 2015*, *2015-July*(1), 113–118. https://doi.org/10.1109/PC.2015.7169947

Vasičkaninová, A., Bakošová, M., & Mészáros, A. (2020). Control of heat exchangers in series using neural network predictive controllers. *Acta Chimica Slovaca*, *13*(1), 41–48. https://doi.org/10.2478/acs-2020-0007

APPENDIXES

Appendix A: MATLAB Simulink Models

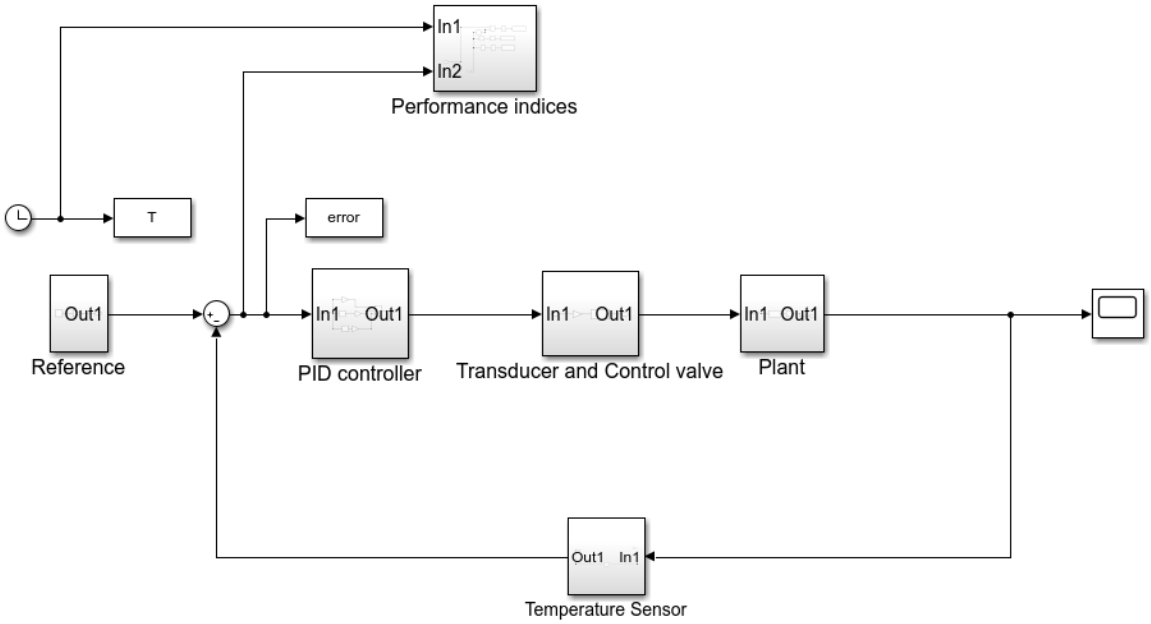

Figure A. 1 Simulink model PID controller under no disturbance condition.

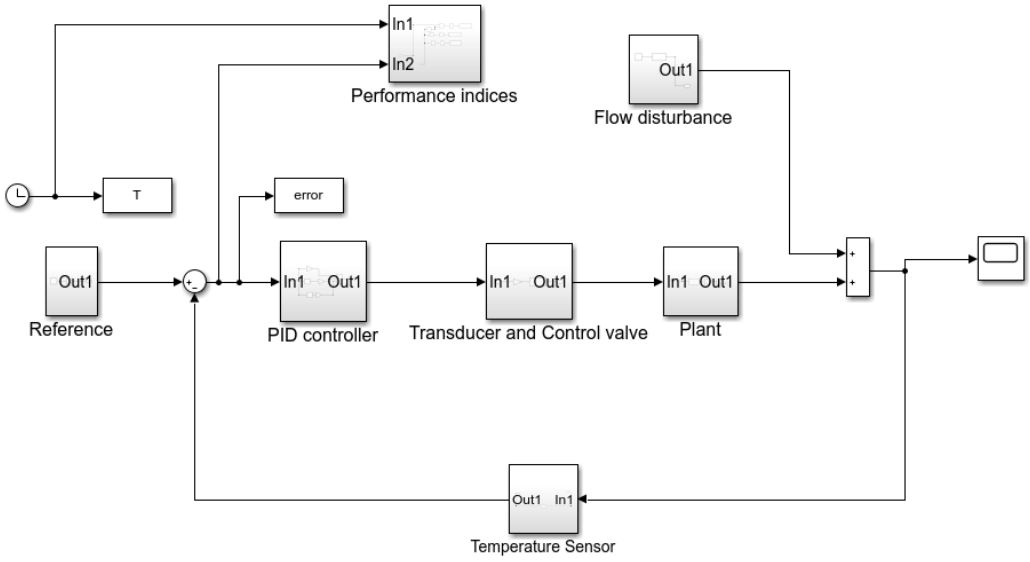

Figure A. 2 Simulink models of PID when the proposed system is subjected to flow disturbance.

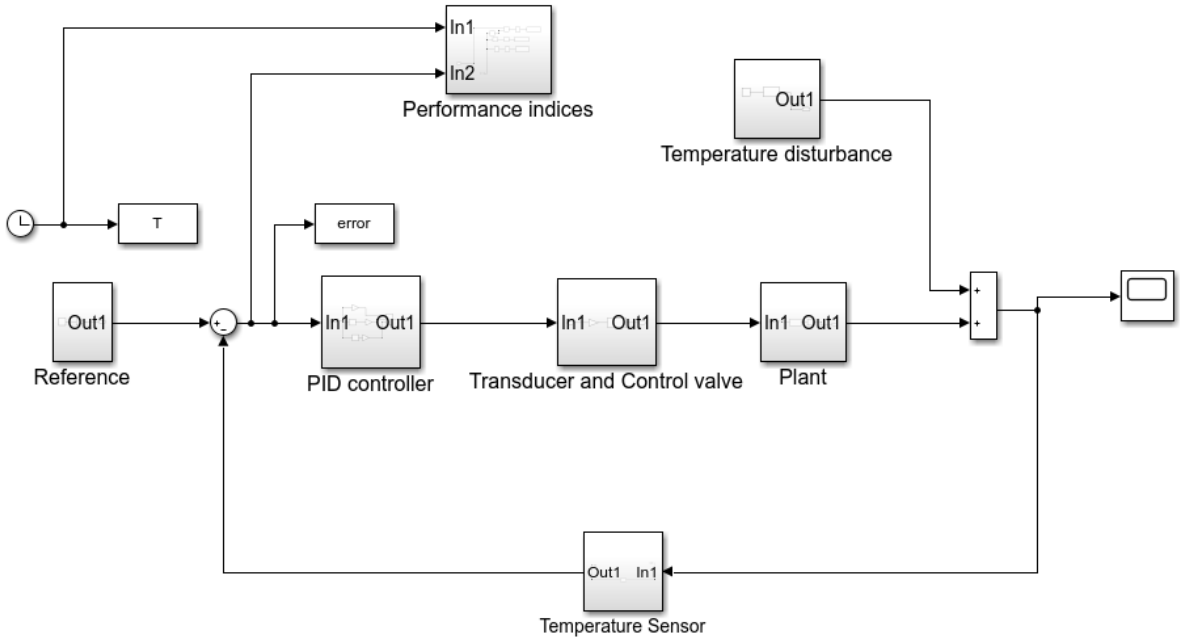

Figure A. 3 Simulink models of PID when the proposed system is subjected to temperature disturbance

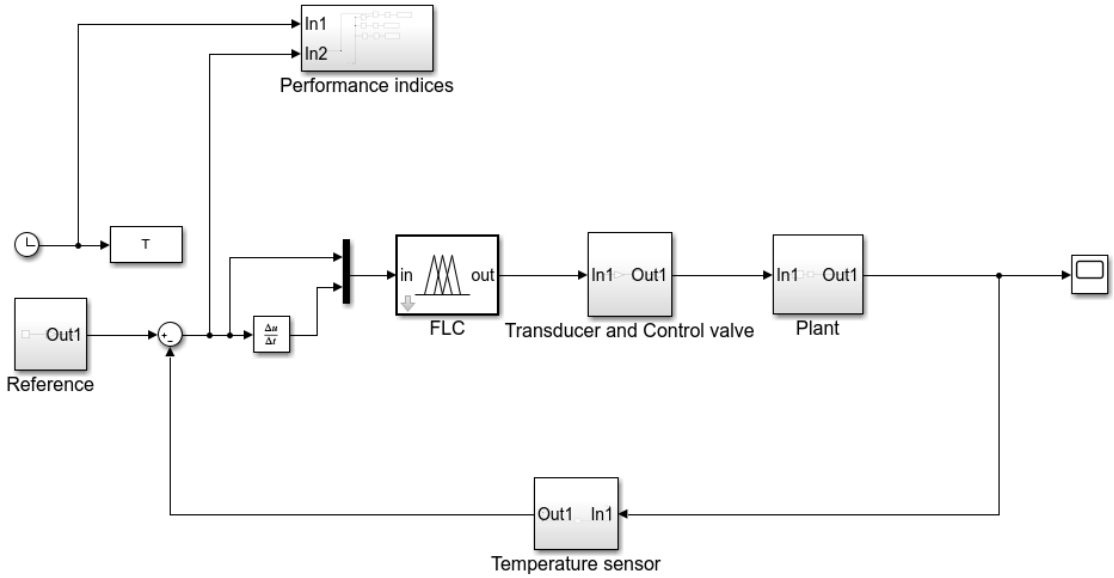

Figure A. 4 Simulink model of the ANFIS PD controller under no disturbance conditions.

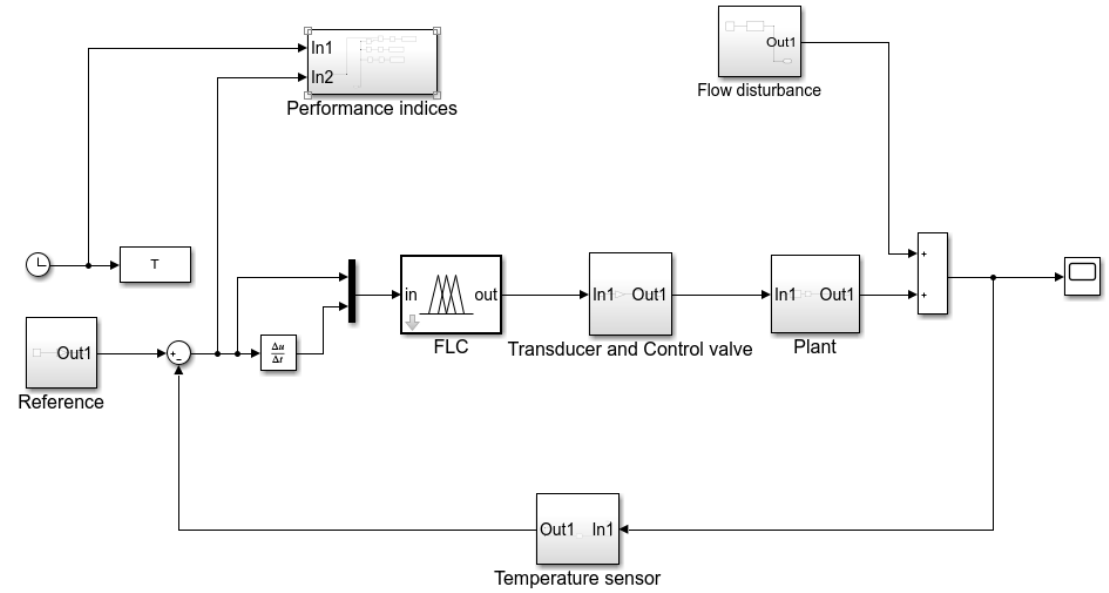

Figure A. 5 Simulink models the ANFIS PD when the proposed system is subjected to flow disturbance.

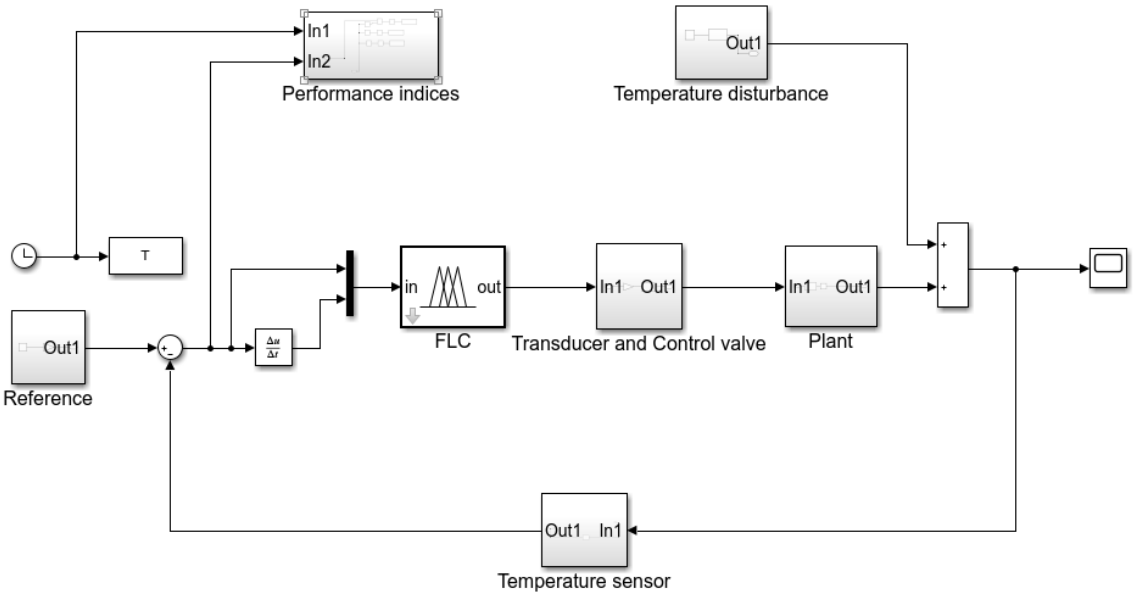

Figure A. 6 Simulink models the ANFIS PD when the proposed system is subjected to temperature disturbance

Appendix B: rule view and surface view of ANFIS

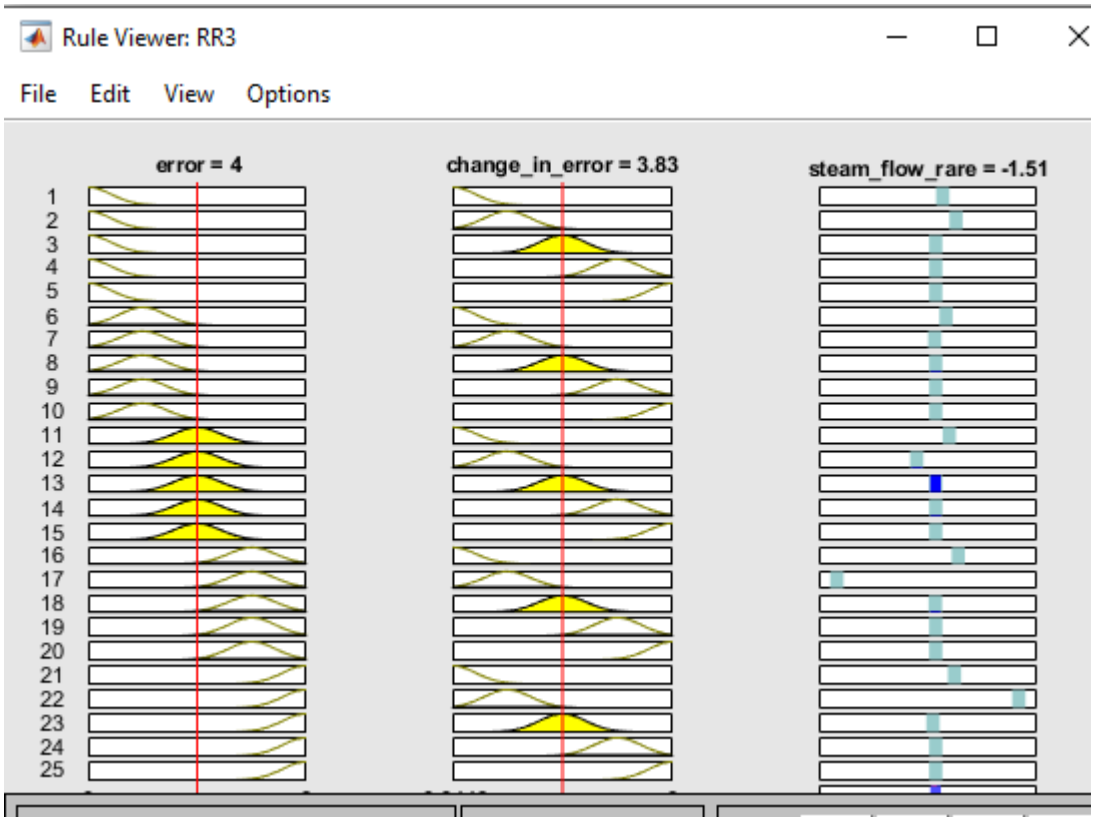

Figure A. 7 Rule view

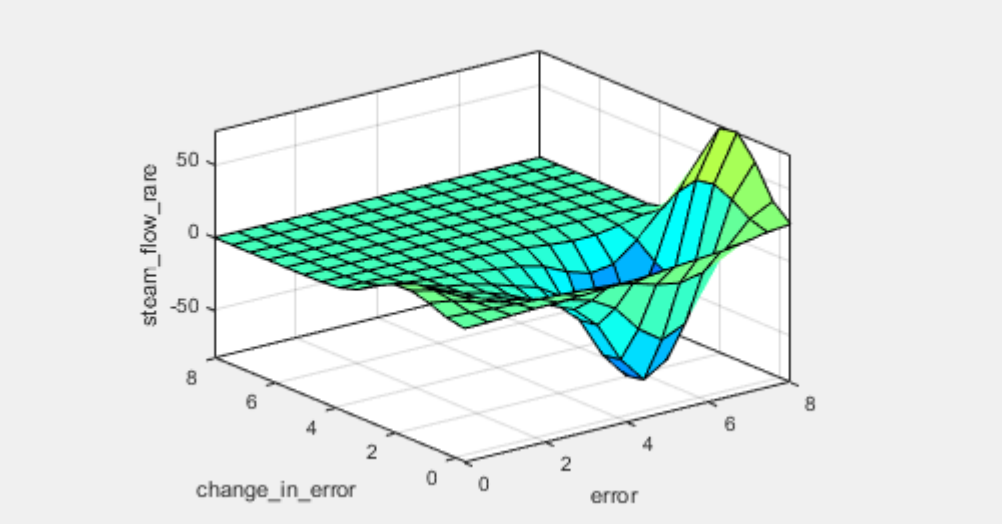

Figure A. 8 Surface view

Appendix C: MATLAB code for the genetic algorithm

```
function GA_PID_gain
options = optimoptions('ga','PlotFcn',@gaplotbestf);
options.PopulationSize = 60;
options.MaxGenerations = 90;
nvar = 3;                    % Number of parameters
  LB = [0 0 0 ];        % Lower bound of tuning parameters
  UB = [10 1 52 ];  % Upper bound of tuning parameters
[x,~] = ga(@EvalObj,nvar,[],[],[],[],LB,UB,[],options);
function obj= EvalObj(x)
simulink_model= 'GA';
load_system(simulink_model);
gains= get_param(simulink_model,'modelworkspace');
 gains.assignin('Kp', x(1));
gains.assignin('Ki', x(2));
gains.assignin('Kd', x(3));
simOut= sim(simulink_model,'SaveOutput','on');
t = simOut.find('time');
e1 = simOut.find('error');
n = length(e1);
%ea = abs(e1);            % IAE
ea = t.*abs(e1);   % ITAE
 %ea = e1.^2;                  % ISE
obj= 0;
for i = 2:n
    stepsize = t(i)-t(i-1);
    obj = obj+0.5*(ea(i-1)+ea(i))*stepsize;
end
```